

## REVIEW ARTICLE

# A rational framework for 3D bioprinting of organoids: From assembly mechanisms and material properties to functional outcomes

**Yuting Wang<sup>1†</sup>, Aizhu Liu<sup>1†</sup>, Yihan Lin<sup>1</sup>, Yun-Long Wu<sup>1\*</sup>, Chiyu Jia<sup>2\*</sup>, and Zheng Luo<sup>1,2\*</sup>**

<sup>1</sup>Fujian Provincial Key Laboratory of Innovative Drug Target Research and State Key Laboratory of Cellular Stress Biology, School of Pharmaceutical Sciences, Xiamen University, Xiamen, China

<sup>2</sup>Center of Burn & Plastic and Wound Healing Surgery, The First Affiliated Hospital of University of South China, Hengyang Medical School, University of South China, Hengyang, Hunan, China

<sup>†</sup>These authors contributed equally to this work.

### \*Corresponding authors:

Zheng Luo  
(zhengl@stu.xmu.edu.cn)  
Chiyu Jia  
(2023010003@usc.edu.cn)  
Yun-Long Wu  
(wuy@xmu.edu.cn)

**Citation:** Wang Y, Liu A, Lin Y, Wu Y-L, Jia C, Luo Z. A rational framework for 3D bioprinting of organoids: From assembly mechanisms and material properties to functional outcomes. *Int J Bioprint*. 2026;12(2):025010539. doi: 10.36922/IJB025010539

**Received:** December 29, 2025

**1st revised:** January 31, 2026

**2nd revised:** February 20, 2026

**3rd revised:** February 28, 2026

**Accepted:** March 6, 2026

**Published online:** April 24, 2026

**Copyright:** © 2026 Author(s). This is an Open-Access article distributed under the terms of the Creative Commons Attribution License, permitting distribution, and reproduction in any medium, provided the original work is properly cited.

**Publisher's Note:** AccScience Publishing remains neutral with regard to jurisdictional claims in published maps and institutional affiliations.

## Abstract

Organoids hold great promise for modeling development, disease, and patient-specific therapy, but their translation is limited by poor vascularization, lack of immune and neural components, low reproducibility, and difficulties in scale-up. 3D bioprinting can address these bottlenecks by enabling digitally guided, spatially precise deposition of bioinks to construct multiscale architectures and perfusable channel networks, yet matching printing principles with material systems remains a central challenge. Unlike existing reviews that focus on isolated technologies or materials, this review introduces a cohesive paradigm that systematically links assembly mechanisms, material properties, and organoid functions along a mechanism–material–function axis. Its core breakthrough shifts the field from empirical guesswork to on-demand engineered design. We analyzed physicochemical mechanisms, such as ionic crosslinking, hydrophobic interactions, dynamic covalent bonding, and photoinitiated polymerization, and mapped them to tunable metrics, including modulus, degradation kinetics, mass-transport capacity, and bioactive delivery. Based on this mapping, we developed a full-chain decision framework for technology selection, material design, and process-parameter optimization, and proposed a predictive, reproducible formulation strategy. By transforming organoid fabrication from an empirical practice into an engineering discipline, this framework enables predictable and scalable organoid fabrication for regenerative medicine, drug discovery, and disease modeling applications through standardized process-parameter optimization and material recipe design.

**Keywords:** 3D bioprinting; Organoids; Bioinks; Crosslinking methods; Bioapplications

## 1. Introduction

Organoids are miniature tissue models formed by the self-organization of pluripotent stem cells (PSCs) or adult stem/progenitor cells under 3D conditions.<sup>1</sup> They can partially reconstruct the cellular composition, spatial structure, and functional characteristics of specific organs *in vitro*, making them extremely valuable for research and translation in fields such as developmental biology, disease mechanism research, drug screening, personalized drug evaluation, regenerative medicine, and precision medicine.<sup>2</sup> However,

current organoid technology still faces many challenges, including the lack of vascularization, immune cells, and neural innervation; insufficient model reproducibility and standardization; and difficulties in large-scale production.<sup>3</sup> Although traditional 3D organoid construction technology is simple to operate, its accuracy is low, and it cannot make organoids as orderly as natural tissue structures, resulting in high heterogeneity between batches and within batches and insufficient reproducibility.<sup>4</sup> Additionally, although organoid chip technology provides a reproducible and controllable method, the complexity of the organoid microenvironment makes large-scale production difficult due to limitations in chip design.<sup>5</sup> Furthermore, as organoids increase in size, the lack of perfusion and vascular-like channels often leads to oxygen/nutrient gradients, hypoxia, and central necrosis, further limiting organoid maturation and the stable integration of multiple cell types/tissue interfaces (immune cells, stromal cells, vascular cells, etc.).<sup>6</sup>

From an engineering perspective, translating these self-assembling cell aggregates into functional tissues that mimic human organs presents significant challenges. Traditional methods, which rely on spontaneous self-organization, often lack precise control, scalability, and functional maturity.<sup>7</sup> 3D bioprinting, smart biomaterials, and microfluidics are emerging as solutions to these challenges, offering the potential for more precise and standardized organoid production. Key obstacles include heterogeneity and repeatability, where variability in size, morphology, and functionality limits consistency.<sup>8</sup> Another critical challenge is vascularization: as organoids exceed 300  $\mu\text{m}$  in size, they face necrosis due to insufficient nutrient supply and lack of perfusable vascular networks.<sup>9</sup> While 3D bioprinting, especially sacrificial coaxial printing, holds promise, current methods still struggle with achieving the required resolution and structural integrity for functional vessels.<sup>10,11</sup> Moreover, controlling the microenvironment is complex, as bioinks must balance printability (e.g., thixotropic properties) with the biological needs of developing tissues. Excessive matrix hardness can hinder soft tissue growth, while overly soft hydrogels may fail to maintain 3D structure during printing.<sup>12</sup> Organ-specific challenges also require tailored strategies, as different organs have unique structures and functions. For example, liver organoids need to replicate compartmentalization and metabolic gradients<sup>13</sup>, while cardiac organoids face challenges in reconstructing myocardial anisotropy and electrical coupling. Brain organoids, with their complex cellular diversity and late-stage maturation hurdles, present the greatest obstacles.<sup>14–16</sup>

In recent years, 3D bioprinting technology has shown

promising applications in organoid manufacturing, enabling better organization of cellular spatial structures and the construction of complex microenvironments and specific physiological characteristics.<sup>17</sup> 3D bioprinting technology enables the precise construction of complex tissue structures by digitally guiding the spatial deposition of bioinks containing living cells, biomaterials, and bioactive factors.<sup>18</sup> From a technical standpoint, different bioprinting modalities rely on distinct assembly mechanisms: for example, extrusion-based printing depends on the shear-thinning behavior of bioinks and on physical crosslinking (such as ionic crosslinking or thermoresponsive gelation)<sup>18</sup>; photopolymerization-based printing employs light-initiated chemical crosslinking (e.g., free-radical polymerization or Thiol-ene click chemistry) to produce high-resolution structures<sup>19</sup>; and embedded printing constructs complex channel networks using sacrificial support materials. These divergent mechanisms determine a subtle balance among material selection, mechanical tunability, and cellular compatibility. For instance, Zhang *et al.*<sup>20</sup> ingeniously combined extrusion printing with dual-source photocrosslinking and, through the concerted design of material mechanics and bioactivity, successfully produced human skin organoids with excellent regenerative performance. Similarly, Skylar-Scott *et al.*<sup>21</sup> improved mass transport in high-cell-density matrices by embedding permeable channels, offering a promising strategy for vascularizing large organoids. Nonetheless, different organoid types have varied requirements in terms of size, cellular composition, and microenvironmental uniqueness. A major unresolved difficulty is choosing material systems that correspond to the specified printing principles. It also necessitates precise control of the bioink's rheology, crosslinking mechanisms, and degradation behavior. Our ultimate goal is to enable multiscale customization, from molecular-level inputs to macroscopic structural organization.

Current research is primarily focused on specialized technologies or material systems, with no systematic design reasoning that unites the chemical mechanics of bioinks, printability, and tissue function. As a result, organoid bioprinting research is still significantly reliant on trial and error, with significant gaps in selecting technical approaches, material compositions, and processing parameters. As a result, research and development cycles are lengthy, and the findings are not repeatable. This review overcomes such restrictions by developing a systematic approach based on fabrication principles. We discussed major hurdles in tissue engineering, such as heterogeneity, vascularization, the microenvironment, and organ specialization. We conducted an in-depth examination

of the physicochemical foundations of various 3D bioprinting techniques. We also examined common 3D bioprinting methods, such as extrusion, droplet-based, and photocuring techniques, as well as the associated bioink crosslinking processes, which might be chemical, physical, or hybrid. These include free-radical polymerization, ionic crosslinking, hydrophobic interactions, and dynamic Schiff base bonding. Furthermore, we related these assembly pathways to critical material performance aspects, such as adjustable modulus, degradation kinetics, and capacity for bioactive molecule distribution (Figure 1). We further related material properties to specific organoid requirements, for example, the need for soft matrices in hepatic constructs, rigid supports for bone-like tissues, and interconnected channel networks for vascularized organoids.<sup>22</sup> By integrating mechanisms, materials, and functions into a unified analytical framework, we offered researchers a comprehensive decision tree that spans technology selection, material design, and process parameter optimization, rather than a collection of isolated techniques. Our ultimate objective is to develop a predictive, reproducible, and standardized formulation that, given key target parameters such as cell composition,

mechanical property range, and structural complexity, yields an optimized bioprinting strategy and material recipe. This paradigm shift aims to transform organoid fabrication from an empirical practice into a controllable engineering discipline and to accelerate translation in regenerative medicine, drug development, and disease modeling.

## 2. Overview of 3D bioprinting technologies for organoid construction

Three-dimensional bioprinting technology simulates the complex structure and composition of human tissues by precisely manipulating the spatial arrangement of cells and bioinks. It overcomes the controllability and uniformity constraints of conventional self-organizing cultures by offering a highly adjustable 3D microenvironment and a repeatable structural basis for organoid production.<sup>23</sup> Presently, 3D bioprinting technologies are primarily categorized into three types: extrusion-based bioprinting, droplet-based bioprinting (DBB), and photocuring-based bioprinting.<sup>24</sup> These technologies utilize different bioinks, where the crosslinking mechanism of the ink directly

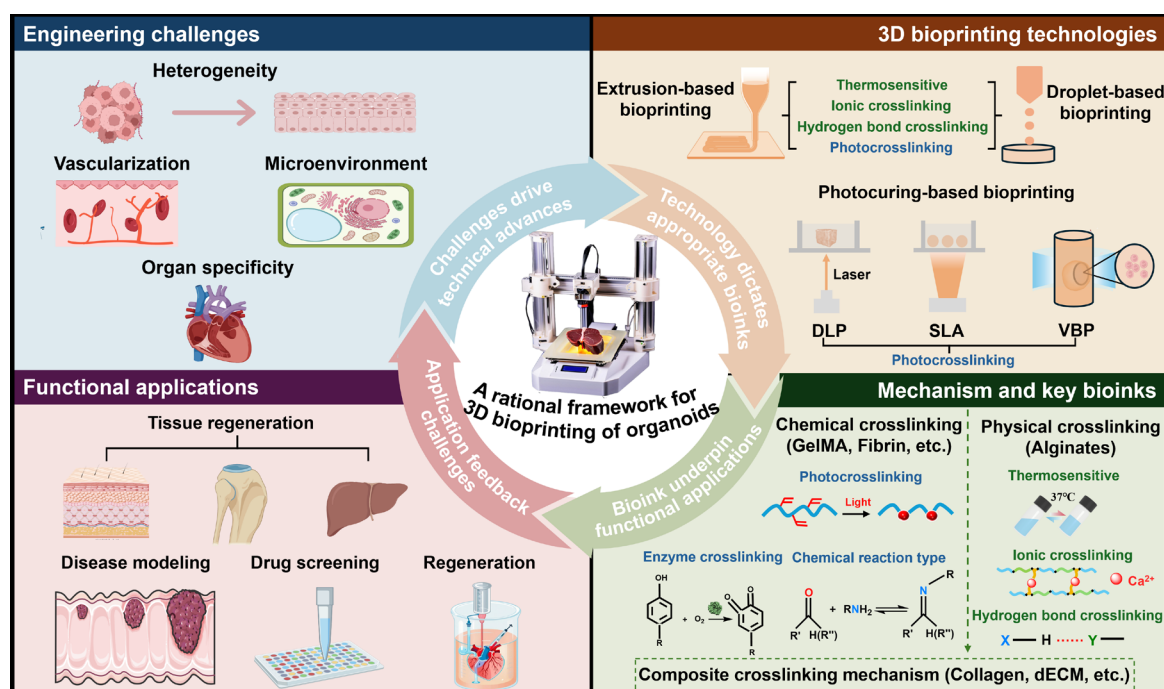


**Figure 1.** Schematic diagram of the rational framework relationship of 3D bioprinting of organoids. This figure meticulously outlines the logical relationships among engineering challenges, 3D bioprinting technology, mechanisms and key bioinks, and functional applications, emphasizing the mechanism–material–function axis that guides predictable and scalable organoid engineering. Created with BioGDP.com.

Abbreviations: DLP: Digital light processing; dECM: Decellularized extracellular matrix; GelMA: Gelatin methacryloyl; SLA: Stereo lithography appearance; VBP: Volumetric bioprinting.

determines printing precision and organoid functional maturation.<sup>25</sup>

The crosslinking mechanisms of bioinks are primarily categorized into two major types: physical crosslinking and chemical crosslinking.<sup>26</sup> Different crosslinking strategies are suited for different printing platforms. Thermosensitive, ionic, and hydrogen-bonded crosslinking are the three main forms of physical crosslinking: Thermosensitive bioinks are often employed to construct breast<sup>27</sup> and fat<sup>28</sup> organoids because they gently gel through temperature changes and are very compatible with extrusion printing; ionic crosslinking bioinks undergo instantaneous solidification via metal cations, enabling immediate shaping in extrusion printing and patterned deposition in droplet printing; and hydrogen-bonded bioinks rely on hydrogen bonding to form dynamic reversible networks, enabling structural retention during extrusion printing and contact-induced curing during droplet printing.<sup>29</sup> They are widely employed for preliminary encapsulation of liver and kidney organoids.<sup>30,31</sup> Chemical crosslinking mainly includes photocrosslinking, chemical reaction (such as Schiff base reaction), and enzymatic crosslinking. Among them, photocrosslinking bioinks undergo rapid and accurate polymerization upon light initiation, making them suitable not only for layer-by-layer curing in extrusion and droplet-based printing, but also serve as the core for achieving integrated solidification in photocuring-based bioprinting. They are frequently employed to construct complex organoids such as brain and kidney models.<sup>32–34</sup> Chemically reactive and enzymatic crosslinking methods necessitate more specific conditions and are frequently used as complementary tactics in extrusion-based printing processes.<sup>35</sup> The following subsections discuss the basics of these three bioprinting methods, their compatible crosslinking methods, and their applications in organoid construction.

### 2.1. Extrusion-based bioprinting

Extrusion-based 3D bioprinting technology is currently the most widely applied and mature bioprinting technique, playing a crucial role in constructing organoids and biomimetic tissues. Extrusion printing continuously extrudes bioink containing cells or organoid units from a nozzle through pneumatic or mechanical pressure, layering it to form 3D structures.<sup>36</sup> Compared to traditional bioprinting technologies, it has several advantages, including low cost, great flexibility, streamlined operation, and increased cell survival. Based on this technique, the world's first commercial 3D bioprinter has been invented.<sup>37</sup>

Extrusion-based 3D bioprinting of organoids generally involves printing pre-cultured organoids or cell spheroids

as “building blocks” alongside a supportive hydrogel. This process allows them to fuse within the printed structure, forming larger tissue constructs.<sup>38</sup> Extrusion printing presents substantial advantages in the construction of large-scale tissues, but shear stress can affect cell viability, requiring the use of shear-thinning bioinks.<sup>39</sup> During subsequent curing operations, thermosensitive physical coagulation or ion crosslinking is commonly used for rapid shaping. Photocrosslinking is also commonly employed for in-situ light curing following extrusion to create a stable culture environment over time (Figure 2A).<sup>28</sup> Based on these characteristics, extrusion-based bioprinting has successfully constructed various organoids, including bone and cartilage<sup>40</sup>, breast<sup>27</sup>, kidneys<sup>41</sup>, hearts<sup>42,43</sup>, and tumors.<sup>44</sup>

To progressively improve the quality of organoid fabrication with extrusion printing, an embedded extrusion printing technique has been invented. This method effectively minimizes shear stress and demonstrates greater tolerance to ink viscosity and flow properties, opening new avenues for constructing extremely biomimetic and complicated organoids.<sup>45</sup> Han *et al.*<sup>44</sup> used embedded extrusion bioprinting to construct colorectal cancer organoids. This model successfully mimics the stiffness and hypoxic conditions of the tumor microenvironment, restoring endogenous and exogenous characteristics while ensuring uniformity. This platform offers a novel strategy for developing morphology-based, label-free drug prediction systems, which is significant for the clinical translation of precision medicine.

### 2.2. Droplet-based bioprinting (DBB)

Droplet-based bioprinting is another nozzle-based bioprinting technology. It includes inkjet, acoustic, electrohydraulic, laser-induced, and microfluidic bioprinting.<sup>39</sup> Inkjet printing is the predominant strategy, which is categorized as continuous or drop-on-demand. These technologies operate by using thermal bubble or piezoelectric actuation to eject low-viscosity bioink containing cells as droplets (at the microliter/picoliter scale) onto a substrate.<sup>46</sup> Because droplet sizes are similar to cell diameters, DBB provides distinct advantages for precise manipulation at the single-cell level.

Organoid construction using DBB involves rapidly and uniformly printing thousands of droplet arrays containing cells or micro-organoids onto culture plates or chips. This approach depends heavily on the bioink's rapid crosslinking capacity (such as ionic or light crosslinking) to accomplish immediate solidification and stabilization of the droplets (Figure 2B).<sup>47</sup> One of the primary applications of DBB technology is the construction of tumor organoids to facilitate research on tumor heterogeneity and high-



throughput screening for personalized drugs.<sup>48,49</sup> Moreover, DBB is frequently employed to construct intestinal<sup>50</sup> and lung organoids. Recently, Yang *et al.*<sup>51</sup> developed an ultra-compact automated organoid printer (OrgFab) that uses microfluidic technology to generate droplets from cell-containing Matrigel suspensions. These droplets are then printed with precision onto multiwell plates to generate organoids, which are screened after cultivation. This device can process ultra-small samples (as low as 5  $\mu$ L), including ion- and light-crosslinked bioinks, with negligible loss. Furthermore, automated and contactless printing improves the efficiency of organoid production. DBB offers exceptional precision and resolution, but it also faces problems such as cell damage caused by shear stress and nozzle clogging. Therefore, the bioink needs to have low viscosity and rapid, controllable rheological responsiveness.

### 2.3. Photocuring-based bioprinting

Photocuring-based bioprinting is a 3D bioprinting technique that uses light irradiation to induce the photosensitive biological ink to harden layer by layer or completely.<sup>52</sup> The entire process takes only a few seconds, or even less, to complete at ultra-high resolution, significantly enhancing the speed and precision of bioprinting. Traditional photocuring-based biological printing mainly includes digital light processing (DLP), stereolithography (SLA), and two-photon polymerization.<sup>53</sup> However, with its development, volumetric bioprinting (VBP) has emerged as an advanced photocuring technology. DLP and SLA technologies use a layer-by-layer curing method, while VBP irradiates the entire volume from numerous angles, allowing for one-step bulk curing.<sup>54</sup> In recent years, photocuring-based bioprinting has emerged as an effective method for manufacturing organoids.

Photocuring bioprinting relies entirely on photocrosslinking bioinks; therefore, choosing photoinitiators and optimizing photocrosslinking parameters are crucial. A balance must be struck between cure efficiency and cellular phototoxicity. Photocuring, unlike traditional bioprinting procedures, does not use nozzles, which eliminates shear forces. This makes it excellent for printing cells that are sensitive to shear stress, such as induced PSC (iPSC) aggregates, or premade organoids.<sup>52</sup> Another advantage of this technology is its ability to construct organoids with complex internal structures, such as vascularized tissues, including those of trabecular bone and meniscus<sup>55,56</sup>, liver<sup>57,58</sup>, and pancreas.<sup>59</sup> Hasenauer *et al.*<sup>60</sup> recently developed a duct/acinar mammary gland model employing VBP, demonstrating *in vitro* lactation function (Figure 2C). VBP overcomes the limitations of layer-by-layer printing for manufacturing

hollow, overhanging structures, making it particularly suitable for constructing perfusable tissues such as those of mammary ducts and alveoli. This technology not only enhances the precision and biocompatibility of printed structures but also mimics the microenvironment of human mammary tissue by modulating the mechanical properties of the material. It provides a controllable and reproducible *in vitro* model platform for studying lactation mechanisms. Overall, photocuring bioprinting offers advantages such as high printing speed, non-contact operation, and enhanced cell viability, opening new avenues for rapid additive manufacturing of organoids. However, it also requires bioinks to have properties such as high transparency and photosensitivity, limiting material selection.

In summary, extrusion, droplet, and photocuring bioprinting technologies, combined with their respective crosslinking bioinks, collectively form a diversified platform for constructing organoids with varying structures, precision, and functions. Table 1 systematically compares the core performance parameters of the three technologies, including printing resolution, cell viability, and forming efficiency, providing a clear basis for technology selection.<sup>61–64</sup> Furthermore, the synergistic combination of fluidic chip technology and 3D cell culture provides a microfluidic platform for bioprinting, enabling high-throughput cell screening and dynamic microenvironment simulation. This greatly enhances the versatility and applicability of organoid manufacturing, enabling a more complete experimental system for regenerative medicine research.<sup>65</sup> For example, Zhao *et al.*<sup>66</sup> employed a 5% sodium alginate (SA)–5% gelatin methacryloyl (GelMA) hybrid ink, first crosslinked with 10 mM  $\text{CaCl}_2$  for 10 min, followed by visible-light curing at 10 mW/cm<sup>2</sup> for 10 s. This composite strategy achieved a hydrogel compressive modulus of  $15.2 \pm 1.5$  kPa, surpassing both single ion crosslinking ( $8.7 \pm 0.9$  kPa) and photopolymerization alone ( $12.4 \pm 1.2$  kPa). Cell viability reached  $91.3 \pm 3.2\%$ , also outperforming single methods ( $78.5 \pm 4.1\%$  and  $85.6 \pm 3.8\%$ , respectively), establishing reproducible parameter standards for organoid construction that balance structural stability and cellular viability (Figure 2D). Moreover, new disruptive 3D bioprinting technologies are emerging: non-invasive photocuring uses near-infrared light and upconversion nanoparticles to accomplish in-vivo penetration printing, opening possibilities for non-invasive repair<sup>67</sup>; the combination of brick assembly concepts with extrusion bioprinting provides novel approaches for building complicated multi-organ systems<sup>68</sup>; and material-free photocuring allows cells to self-crosslink, resulting in the direct construction of high-density organoids.<sup>58</sup> In the future, the integration of different printing technologies, the development of smart, responsive bioinks, and 3D

Table 1. Performance comparison across the three main bioprinting technologies

Parameter	Extrusion-based bioprinting	Droplet-based bioprinting	Photocuring-based bioprinting
Printing resolution ( $\mu\text{m}$ )	100–500	20–500	10–200
Cell vitality (%)	40–95	>90	>75
Molding speed/efficiency	High	Medium or low	Extremely high
Key advantages	<ul style="list-style-type: none"> <li>Broad biocompatibility</li> <li>Supporting high cell loading</li> <li>Cost-effective and scalable</li> </ul>	<ul style="list-style-type: none"> <li>High printing resolution</li> <li>Precise spatial deposition</li> <li>Robust multimaterial integration</li> </ul>	<ul style="list-style-type: none"> <li>High printing resolution and precision</li> <li>Non-contact</li> <li>Fast printing speed</li> </ul>
Limitations	<ul style="list-style-type: none"> <li>Shear-induced cell damage</li> <li>Limited printing precision</li> <li>Structural instability at a large scale</li> </ul>	<ul style="list-style-type: none"> <li>Nozzle clogging susceptibility</li> <li>Limited cell loading capacity</li> <li>Restricted material compatibility</li> </ul>	<ul style="list-style-type: none"> <li>Phototoxicity concerns</li> <li>High operational cost</li> <li>Limited deep curing capability</li> </ul>

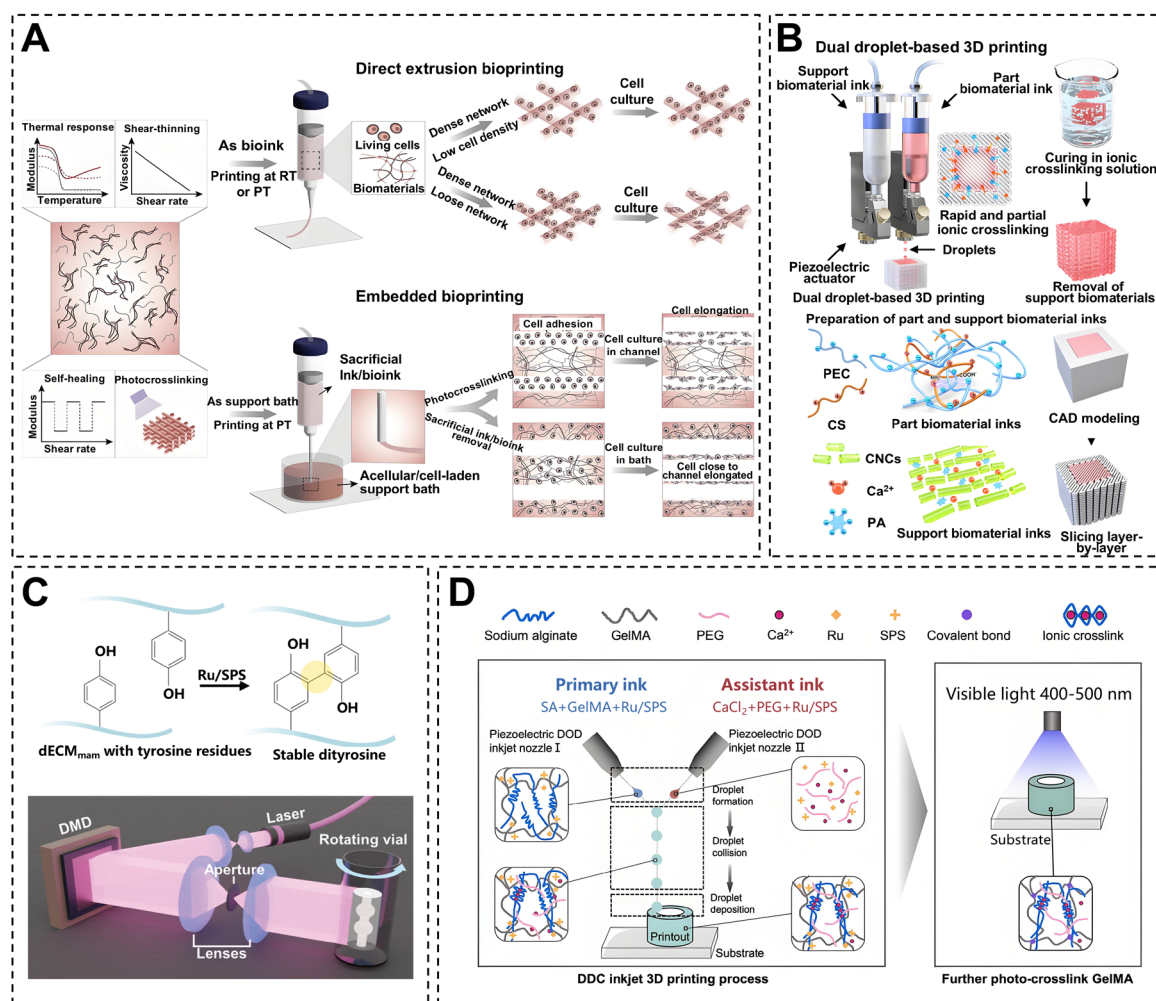


**Figure 2.** Schematic diagrams of 3D bioprinting techniques and their crosslinking mechanisms for organoid construction. (A) Extrusion-based bioprinting. Reprinted with permission from Wang *et al.*<sup>28</sup> Copyright © 2025 Elsevier. (B) Droplet-based bioprinting. Reprinted with permission from Hwang *et al.*<sup>47</sup> Copyright 2025 Elsevier. (C) Photocuring-based bioprinting. Reprinted from Hasenauer *et al.*<sup>60</sup> (D) Combination of multiple printing technologies. Reprinted with permission from Zhao *et al.*<sup>66</sup> Copyright 2025 Elsevier B.V.

bioprinting for personalized medicine will be critical drivers propelling bioprinted organoids toward greater bionic fidelity, throughput, and clinical translation.

The choice of bioprinting process affects structural formation, whereas tissue function is ultimately determined by material properties. Material design for bioinks is the critical link between physical printing restrictions and biological requirements. Various crosslinking methods directly control the rheology, stability, and biocompatibility of the ink, dictating its applicability for specific printing procedures and altering tissue function. As a result, rational ink design requires a clear, logical chain that connects crosslinking methods to material attributes, printing compatibility, and functional output.

### 3. Key bioink materials and their crosslinking mechanisms for 3D organoid bioprinting

This section conducts an in-depth analysis of bioink systems based on three primary mechanisms: physical crosslinking, chemical crosslinking, and composite crosslinking. It provides detailed explanations of the composition of various materials, their gelation principles, mechanical properties (e.g., stiffness and rheology), biological effects, and cutting-edge applications in specific organoids. To translate these standards into organoid-specific design choices, we linked printing/assembly mechanisms to material selection, key performance features, and final functions and biological applications, and summarized representative 3D-bioprinted organoid systems in [Table 2](#).

#### 3.1. Characteristics of ideal materials in 3D bioprinting

##### 3.1.1. Printability

Cells, precursors, or organoid modules must be deposited within a predefined 3D structure with bioink (such as hydrogels) during the organoid printing process. Poor printability (such as inappropriate rheology, unstable deposition, poor interlayer adhesion, and rapid structure collapse) makes precise spatial control difficult, and tissues with complex topologies, microchannels, or heterogeneous cell distributions are impossible to construct.<sup>69</sup>

During the printing process, the material must have an efficient flow–deposition–curing–support chain. It should be simple to extrude or spray. It must swiftly regain its original structural shape after deposition to avoid diffusion, collapse, or deformation. It also needs to maintain the geometry and microenvironment after printing. This ensures the organoids have a stable developmental environment. High-throughput and highly repeatable

printing is also required for scaling up organoids, and poor printability makes standardization difficult.<sup>70</sup>

In summary, printability is the first step toward realizing designer type organs (rather than merely self-organizing organs), and it is the crucial starting point for materials to progress from “usable” to “engineerable”.<sup>54</sup>

##### 3.1.2. Biocompatibility

Organoid printing is more than just about printing structures. The key is to enable cells or stem cells to survive, multiply, self-organize, and function within the material. If the material is highly poisonous, produces hazardous compounds, or triggers strong immunological or inflammatory reactions, organoids will not develop or mature.<sup>71</sup> The use of materials in the cellular domain must allow cell attachment (or appropriate suspension), migration, differentiation, and intercellular communication, while preventing cell stress or death.<sup>72</sup>

Long-term cultivation of organoids often takes many days to weeks. Materials must be stable and not collapse or fall off due to precipitation, contraction, or deformation. If the biocompatibility is inadequate, it will limit the success rate of organoid formation, functional maturity, or the reproducibility of the investigations.<sup>73</sup>

Material biocompatibility is critical for future applications, such as transplantation and drug screening, to ensure safety and clinical feasibility. It must promote functional integration while minimizing negative immunological reactions.

##### 3.1.3. Bioactivity

The advantage of organoids is their 3D structure and ability to partially replicate organ functions, such as intestinal absorption, liver metabolism, and brain network activity. Materials cannot be used solely as mechanical scaffolds to achieve this. They must provide proper biochemical signals, adhesion sites, and a reversible microenvironment. These properties help stem cells aggregate, self-organize, differentiate, and function.<sup>74</sup>

Bioactive materials (including the cell adhesion peptides arginine–glycine–aspartic acid [RGD], matrix metalloproteinase [MMP] degradation sites, and releasable growth factors) can replicate cell–matrix interactions and encourage organoid development. The lack of bioactivity may lead to organoids remaining immature, having limited functionality, or becoming unsustainable.

Furthermore, bioactivity includes the ability of the material to support the generation of extracellular matrix (ECM) and to respond to cell signals, allowing for dynamic interactions between the scaffold and cells. This

is particularly important for functionalized organoids.<sup>75,76</sup>

#### 3.1.4. Degradability

Although printed materials provide initial support, in an ideal scenario, organoids would gradually disengage from the external scaffold and attain autonomous growth. The material's degradability allows it to disintegrate and release space over a sufficient period, allowing cells to produce their own ECM, expand autonomously, or integrate with host tissues.<sup>77,78</sup> If the scaffold does not degrade sufficiently over an extended period, it may impede cell migration, tissue maturation, and functional development. In contrast, if the degradation occurs too quickly, the structural support fails, the long structure collapses, and the organoids scatter. The synchronization of the degradative rate with the developmental rhythm of the organoids is particularly critical.<sup>79</sup>

In transplantation or *in vivo* applications, degradability considers the material's final biological clearance, safety, and the absence of long-term residues and fibrosis. As a consequence, while printing organoids, particularly at the clinical translation stage, the material's degradability becomes a key design criterion.

#### 3.1.5. Mechanical strength

The mechanical properties of the ECM, like stiffness and viscoelasticity, play an important role in regulating cellular function. 3D bioprinting requires stringent shape fidelity and structural integrity. Mechanically adjustable hydrogels meet these requirements by precisely simulating their mechanical properties using rational material composition and crosslinking design. This ensures sufficient mechanical strength to maintain the 3D structure and mechanical performance during extrusion or DLP printing.<sup>80</sup> Specifically, stiffness modulation creates a stable static network by altering the covalent crosslinking density, such as crosslinker concentration or polymer chain length, thereby providing initial support for the printed structure. In contrast, viscoelastic regulation is based on the introduction of reversible bonds, such as hydrogen bonds or metal coordination, allowing energy dissipation, network reconfiguration, and strong interlayer fusion in printed filaments.<sup>81</sup> Depending on the substance, natural hydrogels, such as decellularized matrices, maintain tissue-specific biochemical signals but lack mechanical strength, necessitating reinforcing solutions. Synthetic hydrogels, such as polyethylene glycol (PEG) and polyacrylamide, have easily separable mechanical properties and scalability, but lack bioactive recognition sites. Hybrid hydrogels, such as GelMA and nanocellulose–collagen composites, strike a balance between printability, mechanical performance, and biological compatibility.<sup>82</sup> Because of the dynamic

adaptability provided by physical crosslinking (reversible non-covalent bonds) and the structural stability provided by chemical crosslinking (irreversible covalent bonds), such hydrogels can withstand deformation during the printing process while providing a microenvironment that provides both dynamic regulatory capacity and long-term structural fidelity for organoid culture.

### 3.2. Physical crosslinking methods for bioinks

#### 3.2.1. Ionic crosslinking

The driving force of ionic crosslinking is electrostatic attraction and coordination complexation between negatively charged carboxyl groups on polysaccharide chains and externally introduced divalent cations (such as calcium ions, barium ions, and strontium ions). Alginate is a natural linear anionic polysaccharide extracted from the cell walls of brown algae (such as *Laminaria hyperborea*). It consists of  $\beta$ -D-mannuronic acid (M-block) and  $\alpha$ -L-guluronic acid (G-block) linked by 1–4 glycosidic bonds.<sup>83</sup> The most notable characteristic of alginate is that the carboxylate anions in its G-blocks can undergo rapid ionic crosslinking reactions with divalent cations (most commonly calcium ions). This process can be described by the “Egg-box model”: the divalent cation specifically binds between the G-blocks of two adjacent alginate molecular chains, coordinating with the carboxyl and hydroxyl groups on the glucuronic acid residue to form a tight chelate structure, thereby instantly transforming the sol into a gel.<sup>84</sup> However, the biological ramifications of these crosslinking kinetics require further investigation, particularly in terms of organoid self-organization.<sup>85</sup> Unlike enzymatic crosslinking, which results in slow network formation, such as in fibrinogen–thrombin complexes, ionic crosslinking causes rapid rigidification. The rapid structural locking results in immediate physical confinement. It can drastically limit cellular motility. It can also prevent the merger of neighboring cell spheroids. This fusion is a dynamic process required for the construction of integrated, larger-scale organoids.<sup>86</sup> While rapid gelation enables high printing quality, it may also inhibit spontaneous cellular reorganization essential for functional maturation. As a result, a precise balance must be maintained between mechanical fixation and biological permissiveness.

Alginate bioink exhibits excellent shear-thinning properties. During extrusion printing, high shear rates cause polymer chains to align along the flow direction, reducing viscosity and protecting encapsulated cells from excessive shear damage. Once extruded from the nozzle, shear forces cease, and viscosity rapidly recovers.<sup>17</sup> As a result of its shear-thinning/rapid recovery profile, alginate



is especially well suited to extrusion-based bioprinting, in which filaments must flow through the nozzle while regaining yield stress shortly after deposition to maintain geometry. Alginate, when combined with rapid ionic crosslinking agents such as  $\text{Ca}^{2+}$ , forms a stable and consistent 3D framework. This framework is ideal for soft-tissue organoid constructs such as liver, intestine, and pancreatic models, which value architectural accuracy and gentle encapsulation. For stiffer tissues, such as tissues in bone, it is more commonly used as a printable carrier for ceramics or inorganic fillers to achieve higher mechanical performance. The storage modulus ( $G'$ ) of alginate gels can typically be adjusted within the range of 0.5–10 kPa, which is suitable for simulating the mechanical conditions of soft tissue environments such as liver, intestinal, and pancreatic organoids (typically ranging 0.1–1 kPa).<sup>87</sup> The formed reticular structure pores are usually between 5 and 200  $\mu\text{m}$  in size, but the pores of natural alginate are more random, which is not conducive to the directional transport of nutrients.<sup>88</sup> Research has indicated that alginate can serve as a matrix for 3D cell culture, supporting organoid formation and functional maintenance. For instance, studies have employed alginate-based bioinks for 3D bioprinting to investigate the osteogenic differentiation of human bone marrow mesenchymal stem cells. Zhou *et al.*<sup>89</sup> prepared a bioink by physically blending SA with halloysite nanotubes (HNTs). Using 3D printing technology and high-temperature sintering processing methods, they fabricated SA/HNTs bone repair ceramic scaffolds that exhibit excellent formability, biocompatibility, and osteogenic activity (Figure 3).

In summary, alginate is more suitable as a basic supporting material for extrusion-based bioprinting with shape stability and tunable mechanics. It is particularly useful for providing an initial 3D framework and repeatable structural fabrication in the construction of soft-tissue organs, such as the liver, intestines, and pancreas. For hard-tissue organs like bone, alginate can also serve as a shaping carrier for inorganic fillers or ceramic inks, enabling the construction of scaffolds with both complex structures and bone repair potential through printing and post-processing.

Alginate has unmatched cell compatibility and on-demand gelation, making it ideal for high-fidelity printing; nevertheless, its rapid locking and low bioactivity may limit spheroid fusion and long-term self-organization. To combine printability with morphogenesis, future innovations should prioritize dynamically programmable/relaxable networks and biofunctionalization (for example, staged gelation, dynamic ion release, and ECM-mimicking

ligands).

### 3.2.2. Thermosensitive gelation

Thermosensitive bioinks utilize temperature changes to induce sol–gel phase transitions, a physical mechanism commonly employed in extrusion-based printing to provide temporary structural support.<sup>90</sup> Xu *et al.*<sup>91</sup> used 3D printing to prepare thermoresponsive N-acryloyl-L-phenylalanine methyl ester (NAPA) hydrogels, providing a new direction for smart medical patches and wearable devices (Figure 4). Gelatin exhibits excellent viscoelasticity and shear-thinning properties, making it an ideal additive for regulating the rheology of bioinks.<sup>92</sup> The printability of gelatin is extremely temperature-sensitive. To achieve optimal extrusion filament shape, the temperatures of the print nozzle and receiving platform must be precisely controlled (e.g., nozzle at 25 °C, platform at 10 °C) to balance flowability during extrusion with setting ability after deposition.<sup>93</sup> Pure gelatin hydrogels rapidly dissolve (sol-gelation) under 37 °C culture conditions and cannot provide long-term physical support for organoids. Therefore, gelatin is typically not used alone as the final scaffold material but rather as a sacrificial template or in combination with other crosslinkable materials such as alginate or GelMA.<sup>94</sup> Unlike alginate, gelatin retains a high concentration of RGD sequences within collagen, significantly promoting cell adhesion, spreading, and proliferation through integrin receptors. Furthermore, gelatin contains MMP-sensitive sites, enabling cells to degrade and remodel the surrounding matrix during development, a process critical for organoid morphogenesis.<sup>93</sup> The stiffness of pure gelatin physical gels is typically low (<5 kPa), making them suitable for soft tissue engineering. However, their structural instability poses a major obstacle during long-term culture.<sup>95</sup> Therefore, thermosensitive gelatin is more suitable as a support for shaping during the printing stage and as a provider of a cell-remodelable microenvironment in organoid bioprinting. It can be used for constructing organoids that rely on matrix remodeling, such as intestinal, pancreatic duct-like, and tumor organoids, and can also serve as a sacrificial template for printing perfusable channels.

In summary, thermosensitive gelatin has excellent extrusion compatibility, shear-thinning printability, and an intrinsic cell-adhesive/metalloproteinase-remodelable matrix; yet, its temperature-dependent physical gel is structurally unstable during long-term organoid growth at 37 °C. Future advances should prioritize composite or two-step stabilizing techniques to preserve remodelability and structural integrity while prolonging the maturation period.



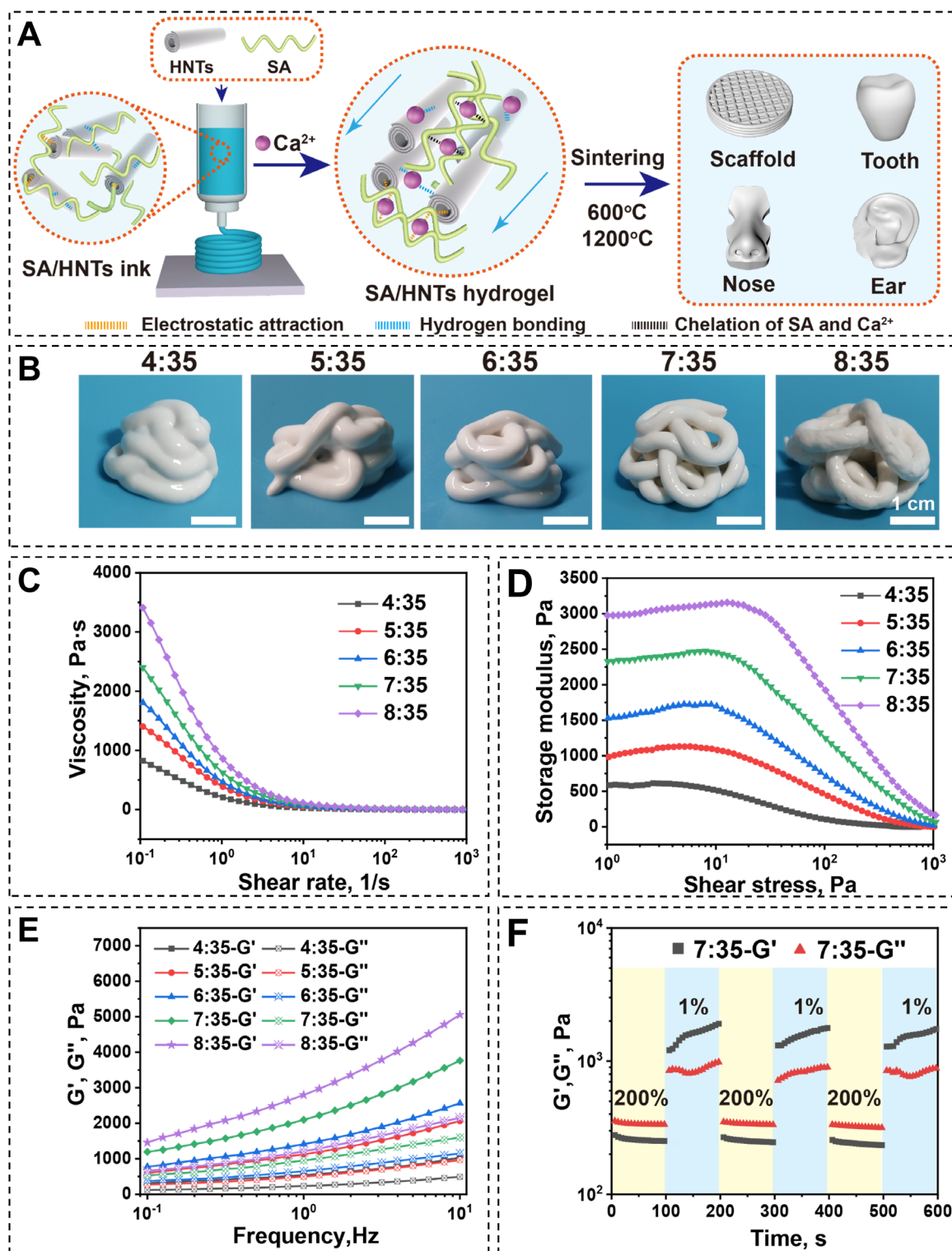


**Figure 3.** Preparation of SA/HNTs scaffolds and rheological properties of sodium alginate (SA)/halloysite nanotubes (HNTs) ink. (A) Schematic illustration of SA/HNT ceramic scaffold preparation. (B) Rheological testing of SA/HNT ink, images of SA/HNT ink at different SA concentrations. (C) Apparent viscosity versus shear rate for inks at different SA concentrations. (D)  $G'$  versus shear stress. (E)  $G'$  and  $G''$  versus oscillation frequency during sweep. (F) Cyclic step strain sweep measurement of 7:35 SA/HNT ink. Reprinted with permission from Zhou *et al.*<sup>89</sup> Copyright 2024 Elsevier Ltd.

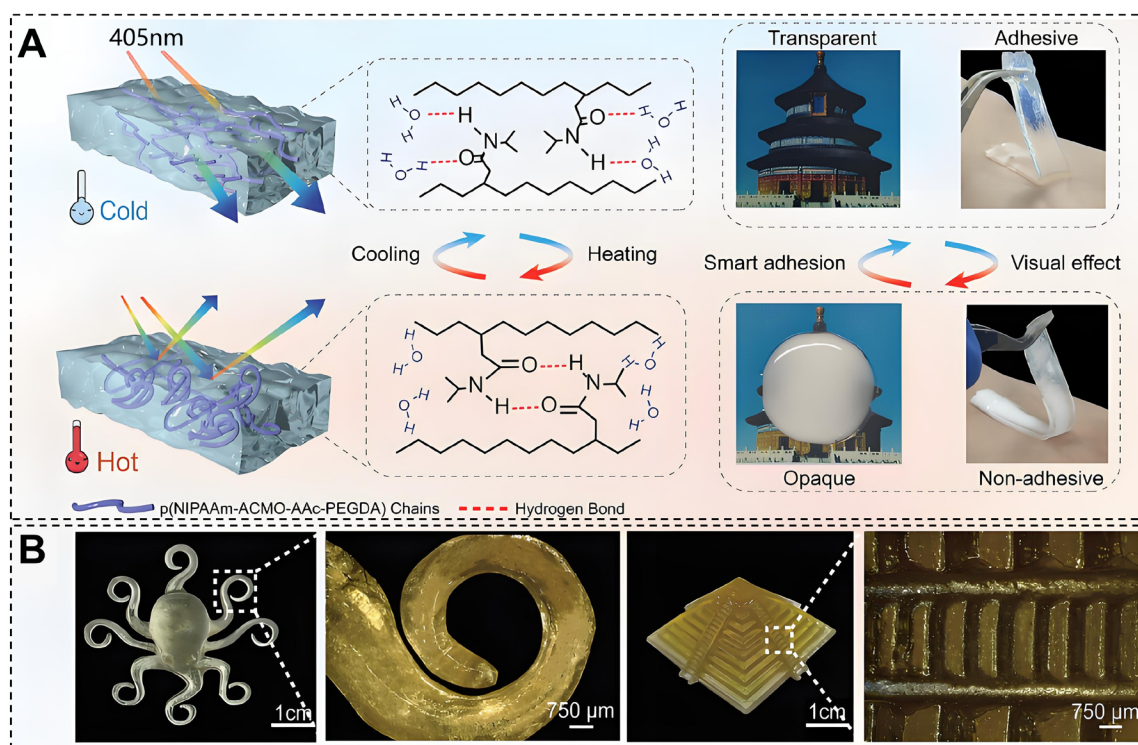


**Figure 4.** Principles and design of thermosensitive hydrogels. (A) Schematic illustration of the mechanism of transparency and adhesion switchable regulation of temperature-sensitive NAPA hydrogel. (B) High-precision hydrogel and structural accuracy display of 3D printing. Reprinted with permission from Xu *et al.*<sup>91</sup> Copyright 2025 John Wiley & Sons.

Abbreviation: NAPA: NacryloylLphenylalanine methyl ester.

### 3.2.3. Hydrogen bond crosslinking

Hydrogen bonds are non-covalent interactions between hydrogen atoms and electronegative atoms (such as O or N) and can occur between groups such as hydroxyl-hydroxyl or carboxyl-amide. The bonding energy of a single hydrogen bond is relatively low, but when a system has multiple sites and dense hydrogen bond donors and acceptors, multiple hydrogen bond clusters can form, acting macroscopically as reversible physical crosslinking points in the polymer network. Such physical crosslinked networks often exhibit the typical shear-thinning and stress recovery/self-healing behavior: under extrusion shear, hydrogen bond clusters can partially dissociate, enhancing chain segment slippage and resulting in lower viscosity, thereby facilitating continuous filament extrusion; after deposition, when shear is released, hydrogen bonds reassociate, reconstructing the network rapidly, helping the filament maintain its shape, and improving interlayer adhesion.<sup>96</sup> Since the entire process usually does not rely on light or highly reactive initiators, it is gentler for cells, making it suitable as a strategy for printing window control in extrusion-based printing.<sup>97</sup>

Pure physical crosslinked networks commonly exhibit low modulus, limited fracture resistance, and insufficient long-term stability, and are therefore more suitable for printing ultra-soft structures (such as brain-like or lung-like soft-tissue constructs) or for combining with a secondary network/secondary reinforcement strategy to enhance structural durability.<sup>98</sup> Hydrogen bonds have never been used alone for 3D bioprinting; however, reports indicate that this strategy has been applied in 3D printing. For example, the diamide groups in poly(N-acryloyl glycineamide) provide physical crosslinking and contribute to strength through hydrogen bonding.<sup>99</sup> Its strength and anti-swelling properties arise from hydrogen bonding between the diamide groups, and it is used in the design of 3D extrusion-printing formulations. In addition, some studies have investigated a high-strength, self-healing, antibacterial, and anti-inflammatory supramolecular polymer hydrogel copolymerized from N-propionylglycineamide and 1-vinyl-1,2,4-triazole.<sup>100</sup> Its network is crosslinked through hydrogen bonds between the diamide groups in the N-propionylglycineamide side chains, without the need for chemical crosslinking agents. This hydrogel exhibits excellent mechanical properties and

can be 3D-printed under simplified hot-melt extrusion conditions to form different shapes and patterns.

Currently, although hydrogen bond crosslinking has shown excellent printability and self-healing properties in 3D bioprinting, it usually needs to be combined with other crosslinking mechanisms, mainly due to common issues of standalone hydrogen bond crosslinked networks, such as low modulus, poor fracture resistance, and insufficient long-term stability. However, with a deeper understanding of the hydrogen bond crosslinking mechanism and material systems, it may be possible in the future to independently use hydrogen bond-crosslinked materials in 3D bioprinting and fully leverage their unique advantages.

### 3.3. Chemical crosslinking methods for bioinks

Physical hydrogels have inherent limitations, such as low mechanical strength and a high disintegration rate. Chemical crosslinking techniques can be used to construct mechanically stable and precisely programmable 3D crosslinked networks that overcome these difficulties. These networks are produced by forming irreversible covalent bonds between polymer chains.

#### 3.3.1. Photocrosslinking

Photopolymerization currently represents the most precise and controllable crosslinking method in bioprinting. Yang *et al.*<sup>101</sup> have greatly advanced the development of related fields, such as regenerative medicine, using multi-material DLP bioprinting to replicate the complex mechanical and structural diversity of natural tissues *in vitro*. At its core, this mechanism utilizes photoinitiators to generate free radicals that attack unsaturated double bonds on polymer chains. Photocurable crosslinking agents used in photopolymerization-based biological 3D printing primarily include polyethylene glycol diacrylate (PEGDA), GelMA, hyaluronic acid methacrylate (HAMA), hydroxyethyl methacrylate (HEMA), and PF127-DA (Figure 5A). Additionally, many molecules lacking double bonds can be converted into photopolymerizable crosslinkers by introducing double bonds through functional groups such as acrylate or methacrylate. These functional groups are typically grafted onto natural polymer backbones through chemical modification. The reaction converts unstable C=C double bonds into a stable C-C single bond network.

Gelatin methacryloyl has become the gold standard material in bioprinting. It is synthesized by grafting photosensitive methacryloyl groups onto lysine and hydroxyl residues along the gelatin molecular chain through a reaction with methacrylic anhydride. In the presence of a photoinitiator, exposure to specific wavelengths (UV

or visible light) generates free radicals from the initiator. These free radicals trigger a chain polymerization reaction of the methacryloyl groups, forming a stable covalent crosslinked network.<sup>102</sup> GelMA bioink perfectly inherits gelatin's thermosensitive rheological properties while possessing photopolymerization capability. During printing, physical gelation at low temperatures (20–25 °C) maintains the shape fidelity of extruded filaments. After printing, chemical crosslinking via light exposure permanently fixes the structure. The success of GelMA lies in its ability to perfectly combine the biological activity of gelatin (the RGD sequence) with the controllability of photopolymerization.<sup>103</sup> When exposed to photoinitiators and specific wavelengths of light (such as 365 nm UV or 405 nm visible light), GelMA can rapidly crosslink and form a stable hydrogel. The core advantage of GelMA lies in its “precise tunability” of mechanical properties. This is achieved by adjusting the concentration of GelMA and/or its degree of substitution.<sup>104</sup> Its stiffness can be precisely controlled within an extremely wide range.<sup>105</sup> The literature reports that its adjustable range covers tissues from extremely soft (0.1–30 kPa) to extremely hard (10–100 kPa).<sup>106</sup> This tunability enables it to precisely simulate the microenvironment of specific organs. For instance, the stiffness of 5% w/v GelMA is 1.6–2.5 kPa, which perfectly matches the physiological stiffness of healthy liver tissue (1.3–1.7 kPa).<sup>22</sup> Therefore, GelMA is one of the preferred materials for 3D bioprinting of liver spheroids and liver models.<sup>107</sup>

Multiple studies have confirmed that liver spheres derived from iPSCs and printed using GelMA bioink can maintain high cell viability and stable liver functions (such as albumin secretion and cytochrome P450 enzyme activity) *in vitro* for a long period (up to 28 days).<sup>108</sup> Zhang *et al.*<sup>20</sup> accelerated full-thickness skin defect repair by 3D-printing GelMA hydrogel human skin organoids. GelMA is also used to construct skin models (Figure 5B).<sup>109</sup> Meanwhile, Ma *et al.*<sup>110</sup> used a GelMA hydrogel as a 3D printing and molding platform, co-loading CeO<sub>2</sub> nanoparticles (antioxidant) and urolithin A (mitophagy activator) to construct a dual-functional hydrogel, achieving a dynamic regulation strategy of “repair first, protect later” (Figure 5C). Moreover, it is often combined with microfluidic chip technology. For example, a 3D-bioprinted “liver-on-a-chip” model using GelMA to support liver spheroids can simulate dose-dependent damage caused by acetaminophen, providing a more physiologically relevant platform for preclinical drug screening. In the construction of skin organoids and skin equivalents, GelMA is also widely used as a “structure-function integrated” bioink. In the research, 8–15% w/v of GelMA is often used to simulate the softer dermis and the



denser epidermal scaffolds, with its compressive modulus ranging from several kPa to over ten kPa, covering the main range of human dermal shear modulus of 0.1–10 kPa, and can well reproduce the mechanical differences between normal skin and early scars.

In summary, GelMA's adaptability and customizable mechanical properties make it an excellent material for building a wide spectrum of organoids, from soft-tissue organs such as liver and skin to potentially tougher-tissue organs such as bone. Its versatility, along with its biological activity, enables the development of sophisticated, highly functional organ models, paving the way for advancements in personalized medicine, disease modeling, and drug testing.

Polyethylene glycol is a biologically inert "blank slate," and its biological activity must be conferred through chemical methods (such as covalent attachment of RGD peptides).<sup>111</sup> PEGDA offers unmatched high reproducibility compared to natural materials, making it ideal for standardization and clinical translation. The stiffness of PEG can be independently adjusted by changing the polymer concentration without affecting its biochemical properties.<sup>112</sup> Its adjustable range is highly suitable for

simulating physiological tissues. For instance, PEGDA at concentrations of 4%, 6%, and 8% has stiffness values of 2.27 kPa, 9.99 kPa, and 25.23 kPa, respectively, covering the range from soft-tissue organs such as the liver to hard-tissue organs such as the heart (10–30 kPa).<sup>113</sup> In terms of pore structure, PEG hydrogels usually exhibit a 3D crosslinked network with a water content of over 90%. The effective pore size ranges from nanometers to sub-micrometers, ensuring the rapid diffusion of small-molecule nutrients, oxygen, and metabolic products. A research team from the University of Virginia in the United States recently published an innovative achievement in the journal *Advanced Materials*: a new type of 3D printing material.<sup>114</sup> This material is compatible with the human immune system and has broad application prospects, especially in the field of artificial organ transplantation. This breakthrough was achieved by modifying the properties of PEG, successfully constructing a highly stretchable network. In summary, PEG and its derivative hydrogel materials not only serve as promising candidates for replacing natural matrices in organoid culture but also provide a highly controllable and standardized platform for elucidating cell–matrix interaction mechanisms, constructing disease models, and advancing the clinical translation of organoids.

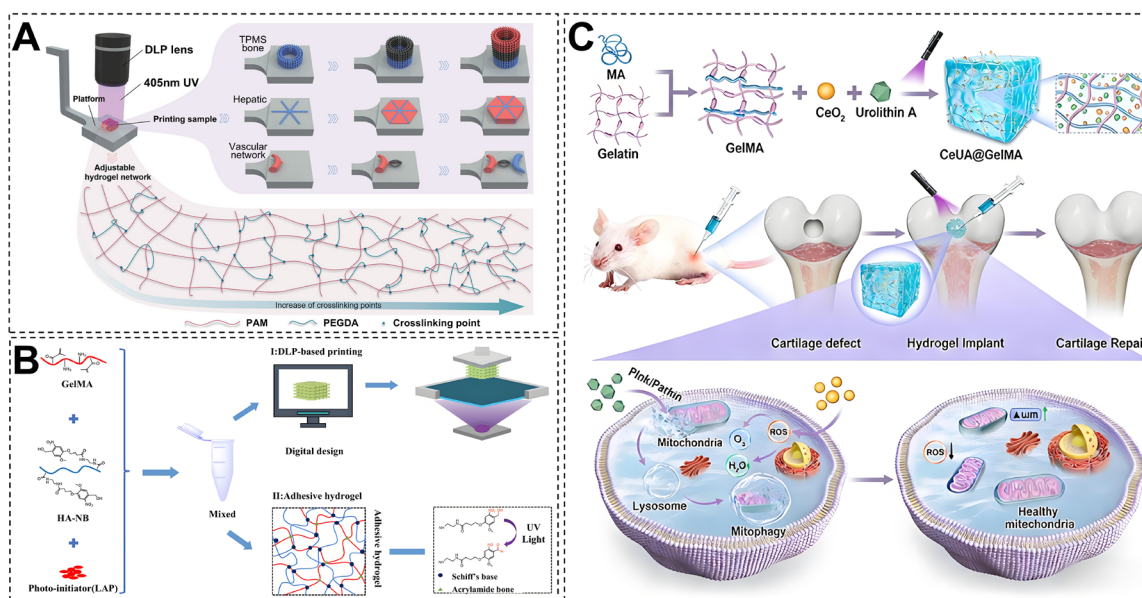


**Figure 5.** Photocrosslinking mechanisms and their application in 3D printing. (A) UV-crosslinked polyethylene glycol diacrylate (PEGDA)–acrylamide (AAM) heterogeneous hydrogels constructing perfusable hollow networks for cells. Reprinted with permission from Yang *et al.*<sup>101</sup> Copyright 2024 Wiley-VCH Verlag GmbH & Co. KGaA. (B) UV-crosslinked gelatin methacryloyl (GelMA)/N-(2-aminoethyl)-4-(4-(hydroxymethyl)-2-methoxy-5-nitrosophenoxy) butanamide (NB) linked hyaluronic acid (HA-NB)/lithium phenyl-2,4,6-trimethylbenzoylphosphinate (LAP) for constructing fast-gelling and mechanically robust hydrogels. Reprinted with permission from Zhou *et al.*<sup>109</sup> Copyright 2020 Elsevier Ltd. (C) Photocrosslinked GelMA/HA-NB/LAP loaded with CeO<sub>2</sub> and urolithin A to construct an adhesive hydrogel for cartilage repair. Reprinted with permission from Ma *et al.*<sup>110</sup> Copyright 2026 Elsevier B.V.

Abbreviation: DLP: Digital light processing; PAM: Polyacrylamide; ROS: Reactive oxygen species; TPMS: Triply periodic minimal surfaces.

Photocurable bioinks provide unprecedented spatiotemporal control and extensive, adjustable mechanical regulation for high-resolution, reproducible organoid production. However, they are still constrained by photoinitiator/light-induced cytotoxicity, curing depth/heterogeneity, and potential stiffness locking, which may limit long-term remodeling. Future development should target more cell-friendly visible/near-infrared photochemistry, resulting in faster and gentler curing while lowering the free radical burden, as well as double-network designs capable of dynamic remodeling to support maturation while preserving precision.

### 3.3.2. Enzymatic crosslinking

Enzymatic crosslinking is usually carried out under mild conditions close to physiological conditions<sup>115–117</sup>, such as room temperature and near-neutral pH<sup>118,119</sup>, which help maintain cell viability and function<sup>120,121</sup>, avoiding damage to cells caused by high temperatures or strong acids and bases.<sup>122–124</sup> This mechanism primarily involves the conversion of fibrinogen to fibrin. The reactive groups are mainly glutamine and lysine residues on the side chains of proteins. The formation of fibrin hydrogels mimics the natural coagulation cascade within the body.<sup>125</sup> Thrombin first cleaves fibrinopeptides A and B from fibrinogen, exposing binding sites that facilitate the physical self-assembly of monomers into protofibrils. These protofibrils subsequently crosslink to form a 3D fibrillar network structure. In the presence of calcium ions, thrombin activates factor XIIIa. Factor XIIIa acts as a transglutaminase, catalyzing an acyl transfer reaction between glutamine and lysine residues on adjacent fibrin chains. This process removes an ammonia molecule, forming a robust covalent crosslinked network.<sup>126</sup> Crucially, the kinetics of this enzymatic crosslinking differ significantly from rapid ionic gelation. The gradual and dynamic network formation avoids the immediate structural locking effect seen in rapid-gelling bioinks, resulting in a permissive microenvironment that promotes cell migration and the fusion of adjacent cell spheroids, which are required for autonomous organoid self-assembly.<sup>127</sup> Consequently, while slow gelation presents manufacturing issues, it maintains the viscoelasticity essential for multicellular reorganization and tissue formation. Fisch *et al.*<sup>128</sup> proposed a novel calcium-triggered enzymatic crosslinking (CTEC) bioink mechanism based on factor XIII activation cascade and applied it to the biomanufacturing of cartilage structures (Figure 6).

Pure fibrinogen solutions typically exhibit low-viscosity Newtonian fluid behavior, lacking the shear-thinning and yield-stress characteristics required for extrusion printing. Direct printing of pure fibrin is extremely challenging and

typically results in structural collapse. Therefore, the fibrin/fibrinogen system lends itself better to DBB and dual-component in situ curing. These methods include multi-nozzle co-deposition and support bath or embedding strategies. Low-viscosity deposition can be stabilized into constructs by fast enzymatic polymerization. Functionally, this printing compatibility is consistent with organoid and tissue models. These models benefit from fibrin's favorable milieu for adhesion, migration, and remodeling. Examples include skin or wound substitutes, vascularized modules, brain tissues, and tumor angiogenesis models. To maintain long-term structural integrity in tissues with strong mechanical demands, fibrin is frequently employed in composite or reinforced networks. Additionally, fibrinogen is frequently printed into a supportive bath that contains thrombin.<sup>129</sup>

Fibrin gel is inherently very soft (typically 0.1–5 kPa), making it an ideal material for soft tissue engineering, such as nerves and blood vessels, but completely unsuitable for weight-bearing organs like bone. Yan *et al.*<sup>130</sup> achieved a milestone by constructing human neural tissue with functional neural circuits using a fibrin-based bioink. They selected fibrin as the base ink precisely due to its low stiffness (0.1–1 kPa), which closely matches the natural mechanical properties of human brain tissue. Using this bioink, they successfully printed and maintained the layered structure of cortical and striatal tissues. Fibrin ink was also used to construct 3D models of tumor angiogenesis. For example, by printing fibrin ink containing human umbilical vein endothelial cells, fibroblasts, and glioblastoma cells, researchers successfully simulated the abnormal morphology and hypoperfusion of tumor vessels.<sup>131</sup>

In summary, fibrin is more suitable for constructing dynamically remodeling soft-tissue organoid models, especially in areas such as brain/nerve tissues, vascularized modules, and tumor angiogenesis, and simulating the microenvironment. However, its poor stiffness and rheological properties make it unsuitable for extrusion, limiting scalable manufacture. Future research should focus on in situ curing of programmable dynamics (e.g., controlled thrombin/factor XIIIa delivery), reinforcement with mixed/composite materials for long-term stability, and the incorporation of perfusable printing workflows to combine bioactivity with robust construct fidelity.

### 3.3.3. Schiff base reactions

The Schiff base reaction is the process by which an aldehyde group (–CHO) forms an imine bond with an amino group (–NH<sub>2</sub>). This is a dynamic covalent chemical reaction.<sup>132</sup> Shear-induced chemical bonds are dynamically reversible and pH-sensitive. Under printing shear forces,



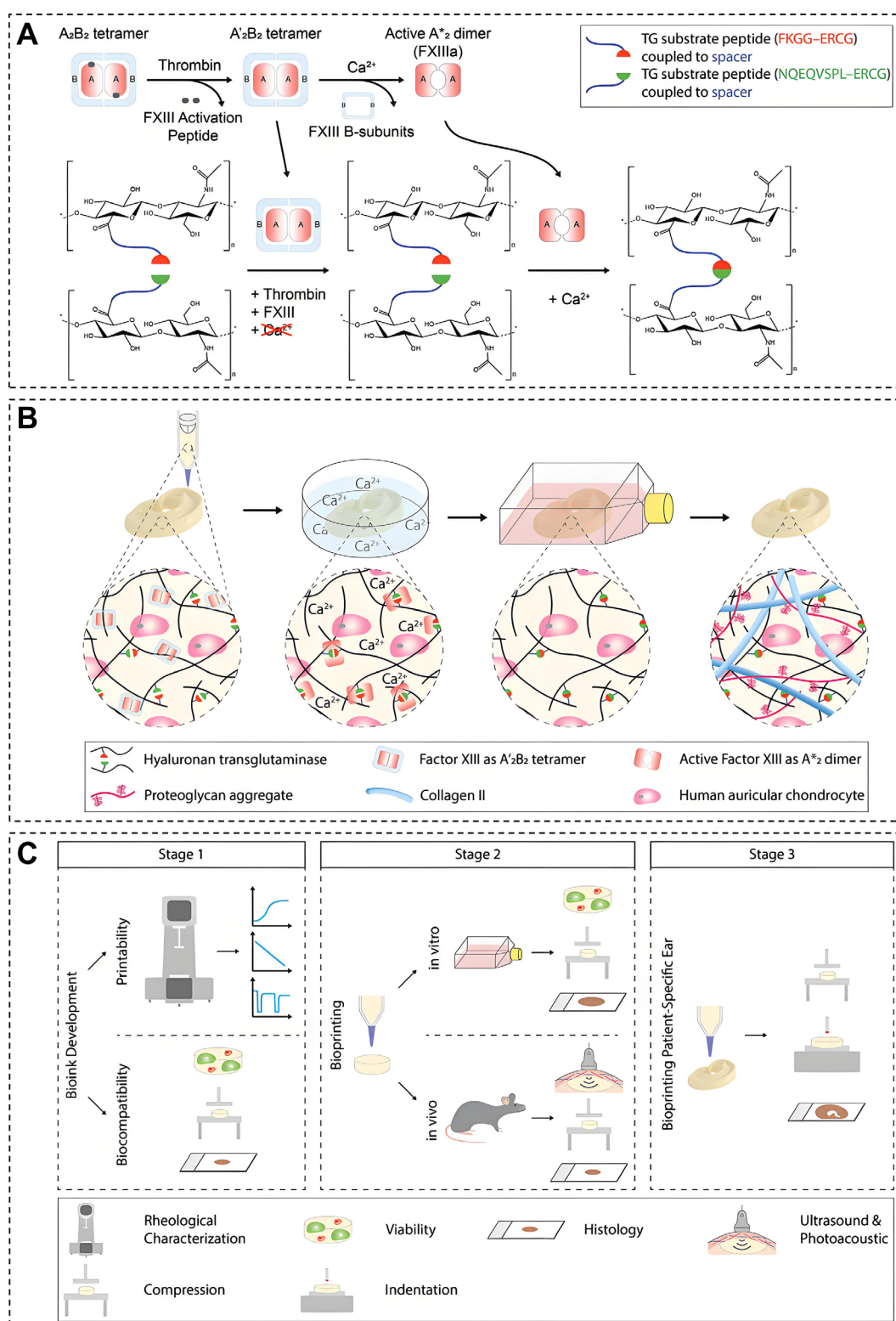


**Figure 6.** Enzymatic crosslinking mechanism and its application in 3D printing. (A) Activation cascade of factor XIII (FXIII). (B) Schematic diagram of the  $\text{Ca}^{2+}$ -triggered hyaluronan transglutaminase (HA-TG) enzymatic crosslinking (CTEC) bioprinting process. (C) The stages of the development of the food chain. Reprinted with permission from. <sup>128</sup> Copyright 2021 Wiley-VCH Verlag GmbH & Co. KGaA.

chemical bond breakage reduces viscosity; post-extrusion, rapid chemical bond reformation enables self-healing and structural stabilization. This mechanism confers exceptional printability to the material without requiring UV light or toxic crosslinking agents.<sup>133</sup> Common combinations include oxidized alginate (introducing aldehyde groups) with gelatin (containing amino groups), or oxidized glucan with chitosan. For example, chitosan/oxidized glucuronic acid hydrogels first form soft gels via a Schiff base reaction, followed by visible-light-induced crosslinking of phenolic groups to further enhance mechanical strength. This strategy ensures printing fluidity while providing the long-term stability required for cell culture<sup>134</sup>, making it particularly suitable for bioprinting skin and wound dressings.

In summary, dynamic covalent hydrogels formed via Schiff base reactions combine the advantages of shear-thinning, self-healing, and the absence of UV or toxic crosslinkers. They can meet the rheological and shaping requirements of extrusion printing and, through a “two-stage curing” strategy, achieve the structural stability needed for long-term culture. Therefore, beyond applications in skin and wound repair, they also have potential as a dynamic bonding and self-healing matrix for epithelial barrier organoids, tumor organoids, and the printing of multi-material complex structures. However, its weak rigidity and rheological properties make it unsuitable for extrusion, restricting scalable manufacturing. Future studies should focus on in situ curing of programmable dynamics, such as controlled thrombin or Factor XIIIa delivery, as well as reinforcement with mixed or composite materials to ensure long-term stability. Furthermore, the use of perfusable printing procedures should be pursued to integrate bioactivity with robust construct integrity.

### 3.4. Composite crosslinking methods for bioinks

Single crosslinking mechanisms often struggle to simultaneously meet the multifaceted demands of bioprinting for rheological properties, mechanical strength, and biological activity. Consequently, composite crosslinking strategies, including dual-network and interpenetrating network approaches, have emerged as the mainstream choice for constructing complex organoids. By integrating physical and chemical mechanisms, the printability and biological performance of materials can be decoupled to achieve an optimal balance.

The alginate–gelatin system is currently the most widely used extrusion-based bioink formulation. It ingeniously combines gelatin’s thermoreversible gelation (physical) with alginate’s ionic crosslinking (physical).<sup>84</sup> During printing (typically at room temperature or

slightly below), the gelatin component (usually 3–10% w/v) provides the primary viscosity and yield stress by forming a physical gel network, preventing extruded filaments from collapsing. After printing, the structure is immersed in a  $\text{CaCl}_2$  solution, where the alginate component undergoes ionic crosslinking, providing long-term structural stability. During subsequent cultivation, the gelatin component may gradually release, increasing the structure’s porosity.<sup>94</sup> The compressive modulus of composite gels typically ranges from 1 to 5 kPa, making them highly suitable for constructing soft-tissue organoids, such as liver, intestine, and tumors. Compared to pure alginate, the incorporation of gelatin provides essential RGD adhesion sites, significantly enhancing early cell adhesion and spreading. This system offers low cost and ease of operation, making it the preferred matrix for constructing large-scale vascularized tissue blocks.<sup>84</sup> A study has shown that embedding HepaRG liver cells into alginate–gelatin hydrogel can form a stable 3D scaffold structure, and this structure can maintain the metabolic functions of the cells and the activity of cytochrome P450 enzymes for a long time.<sup>135</sup> Zhang *et al.*<sup>136</sup> combined extracellular vesicle mimics derived from M2 macrophages with alginate and gelatin to develop a bioink. This bioink was used in 3D bioprinting to fabricate scaffolds. These 3D-printed scaffolds can be implanted subcutaneously or applied directly to wounds for treatment. Wang *et al.*<sup>137</sup> used the alginate–gelatin system to construct a cartilage–bone bilayer scaffold, thereby achieving the coexistence of the cartilage layer and newly formed cartilage (Figure 7). Furthermore, composite inks are also used to develop a model simulating liver steatosis. By adjusting the viscoelasticity of the hydrogel, the mechanical properties of the diseased tissue can be simulated.<sup>138</sup> The hardness of this composite material can also be adjusted to be close to the liver ECM (1–2 kPa), and the pores can be increased to 50–300  $\mu\text{m}$ , which is more conducive to the formation of bile duct-like structures or vascular precursors.<sup>139</sup> This adaptability enables alginate–gelatin hydrogels to have extensive application potential in tissue engineering and organoid cultivation, providing cells with an appropriate mechanical environment and structural support.

The GelMA–fibrin system combines GelMA’s tunable mechanical strength (chemically crosslinked) with fibrin’s exceptional biological activity (enzymatically crosslinked), forming a semi-interpenetrating polymer network. In this approach, fibrinogen is premixed with GelMA, and thrombin is introduced during or after printing to initiate fibrin polymerization. Simultaneously or subsequently, UV exposure is applied to trigger GelMA polymerization.<sup>126</sup> This composite system addresses the challenges of pure GelMA being difficult to print at extremely low

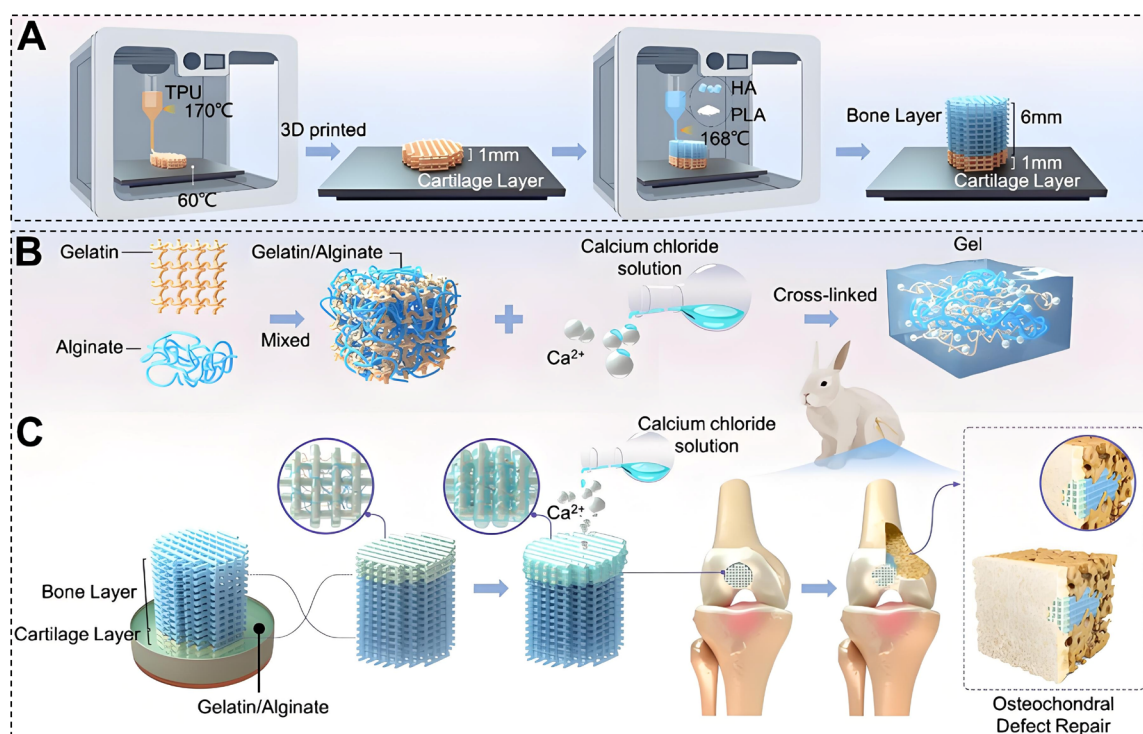


**Figure 7.** Schematic illustration of osteogenic and chondrogenic investigation. (A) Preparation of bilayer scaffold. (B) Preparation of gel. (C) Fill the pores of the cartilage layer of the printed scaffold with hydrogel, and implant the double-layer scaffold into the osteochondral defect area. Reprinted with permission from Wang *et al.*<sup>137</sup> Copyright 2025 Elsevier B.V.

Abbreviations: HA: Hydroxyapatite; PLA: Polylactic acid; TPU: Thermoplastic polyurethane.

concentrations due to excessively low viscosity and the insufficient mechanical strength of pure fibrin. GelMA provides physical support (with tunable stiffness) to protect fragile neural stem cells, while the fibrin network offers an optimal microenvironment for neurite outgrowth and synaptic connections. Research has demonstrated that this composite material effectively supports the development of iPSC-derived neurospheres into mature neuronal networks while maintaining exceptionally high cell viability during the printing process.<sup>129</sup>

In applications such as skin organoids and wound repair, fibrin/fibrinogen-based bioinks are particularly important due to their strong coupling with the coagulation cascade. Taking the fibrinogen–alginic acid composite system as an example, the synergistic effect of fibrin polymerization triggered by thrombin and the  $\text{Ca}^{2+}$ -mediated crosslinking of alginic ions can result in hydrogels with shear-thinning behavior, excellent printability, and a compressive modulus of 1–5 kPa, which are suitable for simulating the mechanical environment of early granulation tissue and the dermis during wound healing.<sup>140</sup> When normal human dermal fibroblasts or human-derived skin organoids are loaded in this type of ink, it is possible to

print out double-layer or full-layer skin equivalents. The cells maintain over 90% viability for 7–14 days and form a dense collagen network and continuous epidermal structure, demonstrating excellent tissue reconstruction ability.<sup>140</sup> Animal experiments further demonstrated that the combined transplantation of human skin organoids and fibrin-based scaffolds could significantly accelerate the closure rate of full-thickness skin defects in mice, could promote orderly vascularization and collagen remodeling, and is a promising strategy for the repair of large-area burn wounds and chronic ulcers.<sup>20</sup> Fibrin-based bioinks not only offer broad application prospects for the construction of skin organoids and wound repair but also provide a bioprinting solution that can be widely applied in clinical treatment through composite hydrogel systems of fibrin and alginate, combined with fibrin polymerization and calcium ion crosslinking. In the future, with the further development of composite materials and secondary crosslinking strategies, the application of fibrin and its related hydrogels will become even more extensive, not only limited to skin regeneration but also expanding to more complex soft tissue repair and organ regeneration.

By combining complementary gelation routes, the

Table 2. Constructing 3D-bioprinted organoids by integrating printing mechanisms, material properties, and functional performance for biological applications

Organoids	Main construction challenges	Recommended 3D materials	Key performance characteristics	Principle of operation	3D printing technology	Application advantages	References
Liver organoids	Reproduce the functional divisions (metabolic gradients) of the liver lobules	GelMA	Stiffness of 1.6–2.5 kPa; matching healthy liver hardness; support long-term albumin secretion and CYP450 enzyme activity maintenance	Chemical crosslinking	Extrusion printing: Constructs cell–matrix composite structures for drug toxicity testing models	Drug screening: Predict the hepatotoxicity of drugs/toxins such as acetaminophen and CCl <sub>4</sub> with performance superior to the 2D HepG2 model	107,108,135,141,142
	Maintain a complex spatial organization and functional polarization	Alginate–gelatin	Stiffness of 1–2 kPa; pore sizes of 50–300 µm; dual crosslinking enhances structural stability; support formation of bile duct-like structures	Physical crosslinking	Photocuring-based bioprinting: Rapidly constructs liver tissue with blood vessels	Disease modeling: Simulate liver steatosis and liver fibrosis, and restore the mechanical properties of the diseased tissues	
	Simulated tubular network	Liver dECM	Contain liver-specific ECM components and growth factors, with a stiffness of 1–5 kPa; induce stem cells to differentiate toward liver cells and enhance the urea synthesis function	Composite crosslinking	-	Personalized medicine: Build models based on patient-derived cells to assess individual drug responses	
	Reproduce the structural anisotropy (ordered arrangement of cells) of myocardial tissue	GelMA	Combined with microfluidic technology; stiffness can be adjusted to 10–30 kPa; support the electrical physiological activities of cardiac muscle cells	Chemical crosslinking	Photocuring-based bioprinting: No shear-force damage, rapidly constructs ventricular-like structures, supports the orderly arrangement of cardiac muscle cells	Regenerative medicine: Develop heart muscle patches with contraction capabilities to repair the infarcted area	
Cardiac organoids (Heart)	Achieve the functional characteristics of syncytia (electrical coupling network)	Cardiac dECM	Stiffness of 5–20 kPa; simulate the normal/fibrotic myocardial microenvironment; promote the contraction function of cardiomyocytes	Composite crosslinking	Extrusion printing (embedded): Reduces shear stress, constructs myocardial tissue with vascular channels	Disease research: Simulate cardiac fibrosis and study the mechanism of abnormal electrical conduction	60,102,143,144
	Construct a large-scale perfusable vascular network to avoid core necrosis	Sacrificial ink (such as Pluronic F127)	Used for printing degradable vascular frameworks and constructing perfusion channels	Chemical crosslinking	-	Drug screening: Assess the effects of cardiovascular drugs on myocardial contraction and electrical activity	

(Cont'd...)

Table 2. Continued

Organoids	Main construction challenges	Recommended 3D materials	Key performance characteristics	Principle of operation	3D printing technology	Application advantages	References
Brain/Neural organoids	Simulate the specific layered structure and regional characteristics of the cerebral cortex	Fibrinogen composite ink	Fibrin promotes nerve differentiation and synapse formation, while GelMA provides mechanical support with a stiffness ranging from 0.1 to 3 kPa, suitable for neural tissues	Chemical crosslinking	Extrusion printing (low shear): Constructs a neural progenitor scaffold and induces its differentiation into a neuronal-astrocyte network	Loop reconstruction: Construct cortical-striatal projections with functional connections to simulate specific neural circuits in the human brain	12,14,16,145,146
	Establish functional neural circuits (long-range projections such as the cortical-striatal projection)	Dynamic crosslinking ink (thiol-ene click chemistry photosensitive gel)	Enable the control of stiffness through light, preventing damage to neural stem cells	Chemical crosslinking	Photocuring-based bioprinting: Rapidly encapsulates iPSC clusters to prevent structural damage	Disease modeling: Study neurodevelopmental/degenerative diseases such as Alzheimer's disease and autism	
	Balancing the flexibility of the matrix with the stability of the printing structure	Low-concentration GelMA ( $\approx 5\%$ )	Relatively low in stiffness but conducive to the extension of nerve protrusions and the formation of vascular endothelial cell networks	Chemical crosslinking	-	Drug testing: Evaluate the effects of neuroregulatory drugs on synaptic formation and electrophysiological activities	
Bone/Cartilage organoids	Simulate heterogeneous cell composition (osteoblasts/osteoclasts/bone cells) and mineralization microenvironment	PCL	Thermoplastic scaffold; porosity of 70–90%; interconnecting pore diameter of 300–500 $\mu\text{m}$ ; compressive modulus of $\geq 0.2\text{ MPa}$ , suitable for the mechanical requirements of cancellous bone	Chemical crosslinking	Extrusion printing: Fused printing of PCL scaffolds, with the implantation of bone-like organs for defect repair	Intracellular regeneration: Bone-healing organoids can achieve bone defect repair within one month after implantation	40,55,56,147
	Re-establish the mechanical load response mechanism	GelMA	Stiffness of 10–20 kPa; promote the mineralization of osteoblasts	Chemical crosslinking	Photocuring-based bioprinting: Rapidly fabricates complex structures such as bone trabeculae and menisci cells	Basic research: Simulate the bone mineralization process and the impact of mechanical load on the activity of bone cells	
	A highly mechanically strong support structure is required to support bone regeneration	Bone dECM	Exhibit excellent shear-thinning properties; significantly increase compressive modulus; support the differentiation of chondrocyte/bone precursor cells	Composite crosslinking	-	Drug screening: Evaluate the effect of anti-osteoporosis drugs on the balance between bone formation and bone resorption	

(Cont'd...)



Table 2. Continued

Organoids	Main construction challenges	Recommended 3D materials	Key performance characteristics	Principle of operation	3D printing technology	Application advantages	References
Kidney organoids	Reproduce complex structures such as glomeruli and renal tubules, as well as their polarity	KdMA (photocoagulated renal dECM)	Crosslinked within 10 s under 405 nm light; with a stiffness range of 0.67–4.81 kPa, they cover the appropriate stiffness range for renal organoids and support the formation of multicellular spheroids	Composite crosslinking	Extrusion printing: Improves the structural consistency and conformational stability of kidney-like organs, and increases the production rate	Toxicity test: Simulate the nephrotoxicity of drugs (such as cisplatin) and predict renal tubular damage	148–152
	The simple dECM has poor printability and is difficult to be formed	Collagen	Stiffness of 20–500 Pa; loose and porous; conducive to the migration of renal tubular epithelial cells	Composite crosslinking	Droplet-based printing: High-throughput fabrication of microarrays of kidney-like organs for toxicity testing	Disease modeling: Reconstruct structural abnormalities such as polycystic kidney disease, and study the pathological mechanisms	
	Lack of a functional vascular network, which restricts the supply of nutrients	GelMA-PEGDA composite ink	The stiffness can be adjusted to 1–5 kPa, enhancing the printing fidelity	Composite crosslinking	-	High reproducibility: Compared to self-organized cultivation, the structural consistency has been improved by over 40%	
	Simulate the heterogeneity of the tumor microenvironment (including stroma, immune cells, and blood vessels)	Gastric-derived dECM (st-dECM)	Retain the specific components of gastric tissue, with a stiffness of 7.5 kPa, simulating the dense matrix of tumors	Composite crosslinking	Droplet-based bioprinting: High-throughput construction of tumor organoid microarrays (such as 96-well plates) for personalized drug screening	Personalized medicine: Predict patients' responses to chemotherapy/targeted drugs, such as the gastric cancer PDO model matching the genetic profile of the primary tumor	
Tumor organoids	Preserve the invasive nature and drug resistance of a patient's primary tumor	Collagen	Stiffness of 20–500 Pa; simulate tumor collagen remodeling; support melanoma cell invasion and T cell infiltration	Composite crosslinking	Extrusion printing (embedded): Constructs colorectal cancer organoids, simulates hypoxia and matrix stiffness, ensures uniformity	Immunotherapy research: Simulate the infiltration and killing of tumor cells by CD8+ T cells, and evaluate the efficacy of immunotherapy	48,51,131,153,154
	Achieve personalized model construction and high-throughput screening	Fibrin	Promote tumor angiogenesis; mimic the abnormal vascular morphology of glioblastoma	Chemical crosslinking	-	High-throughput screening: Simultaneously test 20+ different drug doses, shortening the screening period	

(Cont'd...)

Table 2. Continued

Organoids	Main construction challenges	Recommended 3D materials	Key performance characteristics	Principle of operation	3D printing technology	Application advantages	References
Intestinal organoids	Reconstruction of crypts-villous morphology and epithelial-mesenchymal interactions	Collagen	Stiffness of 20–500 Pa; pore sizes of 1–100 µm; after optimizing crosslinking (tannic acid), they form a cavity-hair structure, with cell viability > 90%	Composite crosslinking	Droplet-based bioprinting: Uses the OrgFab printer to handle samples as low as 5 µL to construct highly accurate lung/colon organoids	Physiological simulation: Form an epithelial structure with absorption function and express intestinal-specific markers (such as K14)	51,139,148,155
	Simulate intestinal absorption function and inflammatory microenvironment	Alginate	Stiffness of 0.1–1 kPa; biologically inert; require combination with gelatin to enhance cell adhesion	Physical crosslinking	Extrusion printing: Constructs intestinal epithelium-matrix composite structures to simulate inflammatory responses	Inflammation model: Simulate diseases such as ulcerative colitis to evaluate the efficacy of anti-inflammatory drugs	
	Cells require extremely soft substrates (with a stiffness of 20–500 Pa) to maintain their polarity	Intestinal dECM	Retain the specific ECM components of the intestine; promote the differentiation of intestinal epithelial cells	Composite crosslinking	-	Drug absorption test: Predict the efficiency of drug absorption through the intestinal tract, replacing animal models	
Breast organoids (mammary glands)	Construct hollow and drooping structures of the ducts/glands to prevent the printing from collapsing	Photosensitive hydrogel (such as GelMA-PEGDA composite)	Highly transparent; photosensitive; with stiffness adjustable to 5–15 kPa, simulating breast tissue	Composite crosslinking	Photocuring-based bioprinting: Non-layer-by-layer printing, one-time formation of duct-acinar structure, achieving ex vivo milk secretion	Functional simulation: Construct a duct-alveolar model with the ability to ex vivo release milk-secretion proteins (such as prolactin)	60,156,157
	Simulate lactation function and the mechanical properties of the mammary gland microenvironment	Breast dECM	Retain breast-specific growth factors; promote differentiation of acinar epithelial cells	Composite crosslinking	Extrusion printing (using ink as a sacrifice): Prints the Pluronic F127 sacrificial framework to construct an injectable catheter	Mechanism research: Investigate the lactation regulation mechanism and the abnormal duct structure during breast cancer progression	
	-	PCL-hydrogel composite scaffold	Provide structural support to prevent the collapse of the hollow structure	Chemical crosslinking	-	Drug testing: Evaluate the effects of breast cancer drugs on breast epithelial cells	

(Cont'd...)

Table 2. Continued

Organoids	Main construction challenges	Recommended 3D materials	Key performance characteristics	Principle of operation	3D printing technology	Application advantages	References
Skin organoids	Simulated dermis-epidermal stratification structure and basement membrane deposition (such as laminin-332)	GelMA (8–15% w/v): Reproduce the mechanical differences between normal skin and scars (stiffness ranging from 0.1 to 20 kPa)	Compressive modulus ranging from several kPa to over 10 kPa; simulate dermis/epidermis; construct vascularized skin chips	Chemical crosslinking	Extrusion printing: Uses sacrificial ink (Pluronic F127) to print vascular channels and constructs a full-thickness skin-equivalent body	Wound repair: Combined transplantation of human skin organoids and fibrin scaffolds accelerates the healing of full-thickness skin defects in mice	20,140,148,158,159
	Reproduce the mechanical differences between normal skin and scars (with stiffness ranging from 0.1 to 20 kPa)	Type I collagen (2–6 mg/mL)	Stiffness ranging from several 10 Pa to several kPa, matching the mechanical properties of the dermis; promote epidermal stratification	Composite crosslinking		Toxicity assessment: Test the percutaneous penetration and irritancy of cosmetics/drugs, replacing animal experiments	

Abbreviations: CYP450: Cytochrome P450; dECM: Decellularized extracellular matrix; ECM: Extracellular matrix; GelMA: Gelatin methacryloyl; KdMA: Kidney-derived methacrylated extracellular matrix; PCL: Poly( $\epsilon$ -caprolactone); PEGDA: Polyethylene glycol diacrylate.

composite system achieves a feasible decoupling of printability and biological functionality, resulting in enhanced shape fidelity and a more cell-friendly milieu. However, its disadvantages include higher formulation and processing complexity, crosslinking heterogeneity, and potential mechanical locking, which could impede long-term remodeling. Future development should focus on standardized, kinetically programmable multi-stage designs with modular bioactive signals and perfusion/vascular integration to support organoid maturation and translation while ensuring reproducibility.

## 4. Functional applications of bioprinted organoids

### 4.1. Tissue regeneration and transplant repair

The core value of organoids in regenerative medicine lies in their role as transplantable sources of functional cells/microtissues for supplementing or replacing damaged tissues, with animal models demonstrating their capacity to repair liver, intestine, and other organoid-derived tissues (Figure 8A).<sup>160</sup> Significant work is being made toward addressing critical translational obstacles. These hurdles include standardized manufacturing, immunocompatibility and safety testing, and scalable expansion.<sup>161</sup> It is important to note that organoids and 3D tissues have advanced from animal validation to early clinical and registration investigations in 2024–2025. Clinical transplantation of iPSC-derived 3D retinal organoids/retinal sheets has been characterized as a typical organoid transplantation in ophthalmology. Patient-focused trials and subsequent safety data have surfaced. According to relevant studies and reports, its clinical feasibility in conditions such as retinitis pigmentosa is being carefully investigated, including immune response, graft survival, and functional endpoints.<sup>162</sup> Furthermore, in gastrointestinal regeneration, a study found that human cell-derived intestinal organoids could repair damaged intestines in rodent models.<sup>163</sup> The report also clearly stated that the next step would be to move on with the first human clinical trial in accordance with Good Manufacturing Practice (GMP) and regulatory standards. This gives a more translationally focused framework for process and safety in intestinal organoid cell therapy.

Compared to traditional cell transplantation, organoids place greater emphasis on maintaining tissue structure and function. However, they remain constrained by bottlenecks such as establishing blood supply post-transplantation, achieving long-term maturity, and overcoming immune rejection.<sup>164</sup> Therefore, providing a suitable microenvironment (matrix/vascularization) and achieving stable integration remain the primary focuses in

this field.

#### 4.2. Pharmacological screening and personalized toxicology

In the drug development process, reliably predicting the efficacy and toxicity of drugs in the human body during the preclinical stage is a key issue that determines the cost and success rate of the research. Traditional 2D cell cultures and animal models often fail to meet the requirements of both human specificity and high-throughput screening (Figure 8B).<sup>157</sup> The liver is the core organ for drug metabolism and toxicity research. The 3D-bioprinted liver organoids provide a solution to this problem that combines physiological relevance and experimental controllability. For example, liver tissue models constructed using bioink containing drugs (such as silymarin) or specific matrix components can reproduce the damage process induced by toxins, such as  $\text{CCl}_4$ , in a 3D environment and quantitatively evaluate the intervention effect of protective drugs.<sup>165</sup> These models are more in line with clinical observations than traditional models in aspects such as the reconstruction of drug metabolism pathways, the dynamic monitoring of cell damage and repair, the analysis of dose-response relationships, and the effects of combined drug use. More recently, humanized 3D-bioprinted livers derived from rapidly reprogrammed human-induced hepatocytes have demonstrated mature hepatic functioning and increased susceptibility to hepatotoxins.<sup>166</sup> They may also capture drug-drug interaction effects. This offers a more patient-specific option for tailored toxicology.

These results indicate that bioprinted organoids have the potential to become a crucial intermediate platform that bridges the gap between cell experiments and clinical trials, enhancing the predictive ability of preclinical screening for the real responses of the human body.

#### 4.3. High-throughput disease modeling and tumor research

Three-dimensional-bioprinted organoids can precisely reconstruct the key microenvironment where diseases develop. They are particularly suitable for modeling complex diseases such as tumors. By printing patient-derived cancer cells together with tissue-specific matrices (such as dECM derived from gastric tissue), researchers have constructed representative models of gastric cancer tumor microenvironments.<sup>154</sup> Using 3D printing technology of hydrogels, *in vitro* co-culture models of tumors were constructed for studies of cell interactions and drug testing (Figure 8C).<sup>142</sup> Unlike traditional 2D tumor cell lines, these bioprinted tumor organoids can better preserve the stromal components, vascular-like structures, and immune cell infiltration characteristics of the patient's

primary tumor in their structure; functionally<sup>167</sup>, they can more accurately reflect the drug resistance, invasiveness, and heterogeneity of tumor cells to chemotherapeutic drugs and targeted drugs; at the application level, they can directly serve as an individualized drug testing platform, enabling parallel evaluation of the efficacy and toxicity of multiple drug administration schemes *in vitro*, thereby providing a basis for clinical formulation of individualized treatment plans. In parallel, high-throughput 3D-manufactured or bioprinted pediatric tumor models, such as neuroblastoma and sarcoma tumoroids, have been incorporated into scalable drug-testing pipelines.<sup>168</sup> These models retain crucial genetic and phenotypic characteristics of the original malignancies. This demonstrates the viability of screening-based bioprinting pipelines for clinically challenging malignancies.

Organoids constructed through bioprinting have shown enormous promise in regenerative medicine, drug screening, and disease modeling. However, its practical implementation still confronts obstacles such as low reproducibility and reliability, largely due to the lack of a standardized framework. To achieve a successful translation from construction to reliable application, a quality control system that spans the entire process, from production to validation, is required. This includes determining the structural consistency, compositional stability, and functional relevance of organoids. The rational framework given herein serves as a theoretical foundation for identifying these important quality features by clarifying the link between assembly procedures, material qualities, and functional outputs. For instance, properly managing the crosslinking kinetics and mechanical characteristics of bioinks provides structural reproducibility, whereas integrating functional microenvironmental cues increases physiological relevance. Consequently, standardization efforts must be anchored on a thorough grasp of structure-function linkages. Resolving this quality control issue is critical to furthering the translational use of bioprinted organoids.

#### 4.4. Multi-organ-on-a-chip and systems toxicology

As the precision of bioprinting technology has advanced from single-type organs to complex integrated systems, multi-organ-on-a-chip has become a key tool for simulating human systemic physiological responses. While traditional single-organ models can replicate the functions of specific organs, they cannot reproduce inter-organ endocrine communication or the systemic pharmacokinetics of drugs.<sup>54</sup> Recent studies have used multi-nozzle bioprinting technology to integrate liver, kidney, intestinal, and heart organoids onto microfluidic chips, enabling perfusion through printed vascular networks.<sup>169</sup>

The research focus in 2025 was on the construction of a fully humanized axis. For example, researchers have developed an intestine–liver–kidney axis model through bioprinting to evaluate the absorption of oral drugs, first-pass metabolism, and renal excretion.<sup>170</sup> Compared with traditional animal experiments, this bioprinted system can more accurately capture secondary toxicity induced by metabolic products. In addition, sensor integration technology allows researchers to monitor fluctuations in oxygen, pH, and metabolic products in the microenvironment in real time. This high-throughput systems toxicology platform not only significantly shortens the drug-screening cycle but also demonstrates unique value in the development of drugs for rare diseases. It can use patient-derived iPSCs to construct human microsystems with specific genetic backgrounds.<sup>171</sup> These iPSCs also provide a foundation for the engineering of various organoids. For example, Lawlor *et al.*<sup>41</sup> used an

extrusion-based 3D bioprinting method to efficiently construct iPSC-derived kidney organoids. These organoids not only formed typical structures of functional proximal tubules but also showed high reproducibility in their cell numbers and viability (Figure 9A). In the study by Li *et al.*<sup>172</sup>, non-genome-integrated, chemically induced human PSCs were used as a reliable cell source to generate highly active and functionally mature hepatic organoids, and their liver-specific functions *in vitro* and *in vivo* were systematically evaluated (Figure 9B). Meanwhile, Skylar-Scott *et al.*<sup>21</sup> proposed an innovative strategy. They used sacrificial hydrogels to construct functional tissues from bioactive matrices, achieving organoids with high cell density, robust maturity, and ideal functionality (Figure 9C). In the future, with the deep integration of bioprinting materials and microfluidic technologies, multi-organ-on-a-chip systems are expected to partially replace non-human primate models in preclinical research and to become a

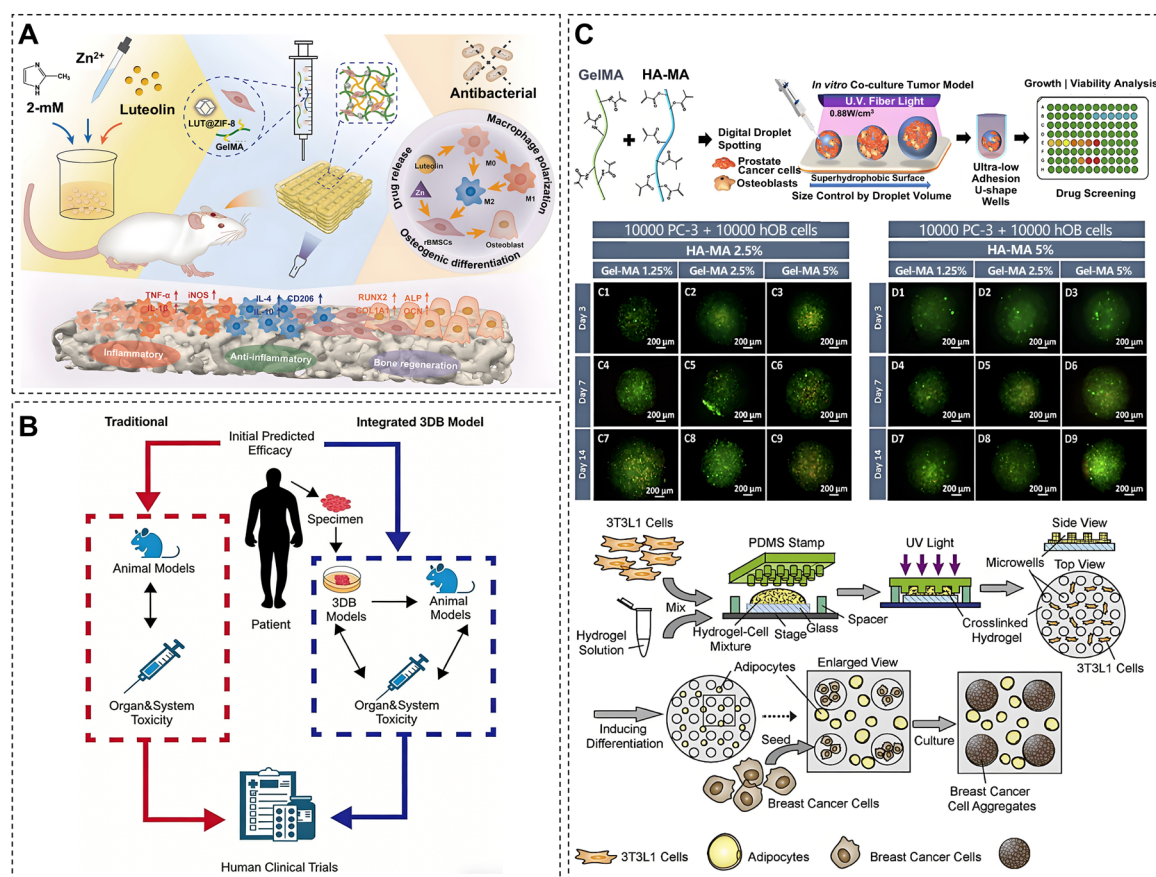


**Figure 8.** Functional applications of bioprinted organoids. (A) Schematic diagram of bone regeneration using bioprinted LUT@ZIF-8/GelMA scaffold. Reprinted with permission from Yu *et al.*<sup>160</sup> Copyright 2025 Elsevier Ltd. (B) Application of 3D-bioprinted models in drug toxicity screening. Reprinted with permission from Ren *et al.*<sup>157</sup> Copyright 2025 John Wiley & Sons, Inc. (C) *In vitro* tumor models for drug screening. Reprinted with permission from Jiao *et al.*<sup>142</sup> Copyright 2024 Elsevier Ltd.

Abbreviations: GelMA: Gelatin methacryloyl; HA-MA: Hyaluronic acid methacrylate; PDMS: Polydimethylsiloxane.



standardized foundation for systems biology studies.

## 5. Conclusion

Traditional organoids rely on self-organization within matrices such as Matrigel, leading to critical bottlenecks, including limited controllability, inconsistent results, high heterogeneity, and a lack of vascular perfusion. This review systematically examines extrusion, droplet, and photopolymerization or volumetric printing techniques alongside compatible crosslinked bioink systems. It emphasizes that spatially precise deposition and digital manufacturing enhance structural reproducibility, and discusses applications in disease modeling, high-throughput drug screening, organ-on-a-chip integration, and vascular network construction.

Looking ahead, 3D bioprinting can advance organoids from “random growth” toward standardized, scalable, and personalized medical platforms.<sup>173</sup> However, three significant obstacles remain. First, routine printing methods

often produce perfusable channels of approximately 100  $\mu\text{m}$ , making capillary-scale vascularization challenging. True capillaries have a diameter of only 6–8  $\mu\text{m}$ , which is difficult to reach. Even the tiniest endothelialized vessels printed to date are in the tens of micrometers range.<sup>173</sup> A possible approach is to print hierarchical macro- and microchannels for rapid perfusion, followed by controlled angiogenic self-assembly to complete the terminal microcirculation using pro-vascular signals and remodeling-permissive matrices. Second, microenvironmental tensions persist over time. Swelling, creep, deterioration, stiffening, and ECM remodeling can all cause mechanical drift, thereby impairing patterning and lumen patency. Meanwhile, mass transport limitations can still induce hypoxia in dense constructs. An effective solution is the use of temporally programmable hydrogels, which decouple the requirements for shape retention during printing from those governing tissue remodeling during culture. The integration of perfusion systems, such as microfluidic chips and integrated vascular systems,

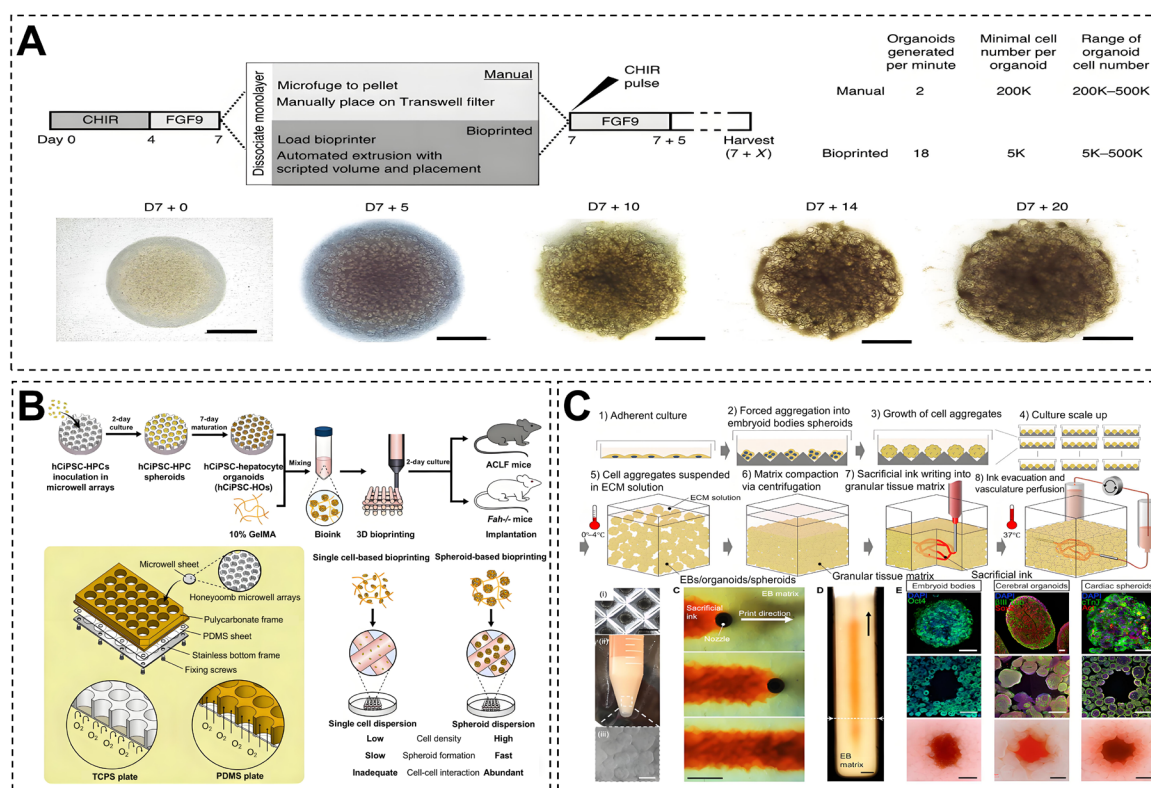


**Figure 9.** Schematic diagram and functional validation of induced pluripotent stem cells (iPSC)-derived bioprinted organoids. (A) Comparison of artificial synthesis and bioprinting for kidney organoid formation and in vivo imaging of bioprinted organoids. Reprinted with permission from Lawlor *et al.*<sup>41</sup> Copyright 2021 Nature Portfolio. (B) Human chemically induced iPSC (hCiPSC)-HPC spheroids matured to hepatocyte organoids (HOs), mixed with gelatin methacryloyl (GelMA), bioprinted as 3DP-HOs to treat two liver failure models. Reprinted with permission from Li *et al.*<sup>172</sup> Copyright 2025 BMJ. (C) Sacrificial writing into functional tissue (SWIFT) process diagram, showing various bioprinted organoids generated by embedding 3D printing in an extracellular matrix (ECM). Reprinted with permission from Skylar-Scott *et al.*<sup>21</sup> Copyright 2019 American Association for the Advancement of Science. Abbreviations: EB: Embryoid body; PDMS: Polydimethylsiloxane; TCPS: Tissue culture polystyrene.

further strengthens this technique. These systems use constant barrier monitoring to ensure that oxygen flows steadily and tissues function appropriately over time. Third, material standardization and system integration remain limited. Matrigel and various dECM preparations exhibit batch variability and unknown compositions, restricting reproducibility and GMP translation. This limitation can be addressed by transitioning to chemically defined matrices with measurable mechanical and biochemical properties, and by employing in-process monitoring and closed-loop control to stabilize deposition and crosslinking across multiple runs. These approaches reduce trial-and-error, minimize batch-to-batch fluctuations, and standardize the printing process, material compositions, and manufacturing parameters, establishing predictable production workflows. Collectively, these strategies streamline the production of stable, clinical-grade organoids from patient-derived cells and facilitate the evaluation of tailored drugs.

## Acknowledgment

The graphical abstract and Figure 1 was created using BioGDP.com (Jiang S, Li H, Zhang L, et al. Generic Diagramming Platform (GDP): A comprehensive database of high-quality biomedical graphics. *Nucleic Acids Res.* 2025;53(D1):D1670-D1676. doi:10.1093/nar/gkae973).

## Funding

This work was supported by the Natural Science Foundation of China (grant number: 82372119), the Fujian Provincial Natural Science Foundation of China (grant number: 2024J02003), and the Health Research Project of Hunan Provincial Health Commission (grant number: 20257724).

## Conflicts of interest

The authors declare no competing interests.

## Author contributions

**Conceptualization:** Yuting Wang, Zheng Luo  
**Resources:** Zheng Luo, Yun-Long Wu, Chiyu Jia  
**Supervision:** Zheng Luo, Yun-Long Wu, Chiyu Jia  
**Writing—original draft:** Yuting Wang, Aizhu Liu, Yihan Lin  
**Writing—review & editing:** Yuting Wang, Aizhu Liu, Zheng Luo

## Ethics approval and consent to participate

Not applicable.

## Consent for publication

Not applicable.

## Availability of data

Not applicable.

## References

1. Zhu Z, Cheng Y, Liu X, et al. Advances in the Development and Application of Human Organoids: Techniques, Applications, and Future Perspectives. *Cell Transplant.* 2025;34:1–20.  
doi: 10.1177/09636897241303271
2. Septiana WL, Pawitan JA. Potential Use of Organoids in Regenerative Medicine. *Tissue Eng Regen Med.* 2024;21(8):1125–1139.  
doi: 10.1007/s13770-024-00672-y
3. Wolff L, Hendrix S. Rethinking Matrigel: The Complex Journey to Matrix Alternatives in Organoid Culture. *Adv Sci.* 2025;12(47):e08734.  
doi: 10.1002/advs.202508734
4. Musah S, Arzaghi H. Unleashing the power of biomaterials to enhance organoid differentiation and function. *Nat Methods.* 2024;21(9):1575–1577.  
doi: 10.1038/s41592-024-02393-5
5. Low LA, Mummery C, Berridge BR, Austin CP, Tagle DA. Organs-on-chips: into the next decade. *Nat Rev Drug Discovery.* 2021;20(5):345–361.  
doi: 10.1038/s41573-020-0079-3
6. Chang M, Bogacheva MS, Lou YR. Challenges for the Applications of Human Pluripotent Stem Cell-Derived Liver Organoids. *Front Cell Dev Biol.* 2021;9:748576.  
doi: 10.3389/fcell.2021.748576
7. Andrews MG, Kriegstein AR. Challenges of Organoid Research. *Annu Rev Neurosci.* 2022;45:23–39.  
doi: 10.1146/annurev-neuro-111020-090812
8. Shrestha S, Lekkala VKR, Acharya P, Kang S-Y, Vanga MG, Lee M-Y. Reproducible generation of human liver organoids (HLOs) on a pillar plate platform via microarray 3D bioprinting. *Lab Chip.* 2024;24(10):2747–2761.  
doi: 10.1039/d4lc00149d
9. Zhang S, Wan Z, Kamm RD. Vascularized organoids on a chip: strategies for engineering organoids with functional vasculature. *Lab Chip.* 2021;21(3):473–488.  
doi: 10.1039/D0LC01186J
10. Nam S-W, Lee H, Jeon D-G, Son M-Y. 3D Organoid Culturing Devices to Induce in Vitro Models of Human Intestinal Inflammation. *Electron Mater Lett.* 2025;21(4):504–512.  
doi: 10.1007/s13391-025-00561-z
11. Gao D, Li R, Pan J, et al. 3D bioprinting bone/cartilage

- organoids: construction, applications, and challenges. *J Orthop Translat.* 2025;55:75–93.  
doi: 10.1016/j.jot.2025.08.008
12. Layrolle P, Payoux P, Chavanas S. Message in a Scaffold: Natural Biomaterials for Three-Dimensional (3D) Bioprinting of Human Brain Organoids. *Biomolecules.* 2023;13(1):25.  
doi: 10.3390/biom13010025
13. Leung MC, Laksman Z. 3D Bioprinting Functional Engineered Heart Tissues. *Int J Mol Sci.* 2025;26(21):10707.  
doi: 10.3390/ijms262110707
14. D'Antoni C, Mautone L, Sanchini C, *et al.* Unlocking Neural Function with 3D In Vitro Models: A Technical Review of Self-Assembled, Guided, and Bioprinted Brain Organoids and Their Applications in the Study of Neurodevelopmental and Neurodegenerative Disorders. *Int J Mol Sci.* 2023;24(13):10762.  
doi: 10.3390/ijms241310762
15. Chen C, Rengarajan V, Kjar A, Huang Y. A matrigel-free method to generate matured human cerebral organoids using 3D-Printed microwell arrays. *Bioact Mater.* 2021;6(4):1130–1139.  
doi: 10.1016/j.bioactmat.2020.10.003
16. Kim E, Jeong E, Hong YM, *et al.* Magnetically reshaping 3D multi-electrode arrays of liquid metals for electrophysiological analysis of brain organoids. *Nat Commun.* 2025;16(1):2011.  
doi: 10.1038/s41467-024-55752-3
17. Huang MS, Christakopoulos F, Roth JG, Heilshorn SC. Organoid bioprinting: from cells to functional tissues. *Nat Rev Bioeng.* 2025;3(2):126–142.  
doi: 10.1038/s44222-024-00268-0
18. Groll J, Burdick JA, Cho D-W, *et al.* A definition of bioinks and their distinction from biomaterial inks. *Biofabrication.* 2018;11(1):013001.  
doi: 10.1088/1758-5090/aaec52
19. Guvendiren M, Molde J, Soares R, Kohn J. Designing Biomaterials for 3D Printing. *ACS Biomater Sci Eng.* 2016;2:1679–1693.  
doi: 10.1021/acsbmaterials.6b00121
20. Zhang T, Sheng S, Cai W, *et al.* 3-D bioprinted human-derived skin organoids accelerate full-thickness skin defects repair. *Bioact Mater.* 2024;42:257–269.  
doi: 10.1016/j.bioactmat.2024.08.036
21. Skylar-Scott MA, Uzel SG, Nam LL, *et al.* Biomanufacturing of organ-specific tissues with high cellular density and embedded vascular channels. *Sci Adv.* 2019;5(9):eaaw2459.  
doi: 10.1126/sciadv.aaw2459
22. Sorrentino G, Rezakhani S, Yildiz E, *et al.* Mechano-modulatory synthetic niches for liver organoid derivation. *Nat Commun.* 2020;11(1):3416.  
doi: 10.1038/s41467-020-17161-0
23. Cui H, Nowicki M, Fisher JP, Zhang LG. 3D Bioprinting for Organ Regeneration. *Adv Healthcare Mater.* 2017;6(1):1601118.  
doi: 10.1002/adhm.201601118
24. Zhang B, Gao L, Ma L, Luo Y, Yang H, Cui Z. 3D Bioprinting: A Novel Avenue for Manufacturing Tissues and Organs. *Engineering.* 2019;5(4):777–794.  
doi: 10.1016/j.eng.2019.03.009
25. Bebian LB, Presa R, Fernandes L, Lourenço BN, Chaudhuri O, Pereira RF. Bioinks with varying densities of physical and chemical crosslinks modulate cellular responses in 3D by altering the viscoelasticity of the cell microenvironment. *Mater Today.* 2025;86:146–161.  
doi: 10.1016/j.mattod.2025.03.019
26. GhavamiNejad A, Ashammakhi N, Wu XY, Khademhosseini A. Crosslinking Strategies for 3D Bioprinting of Polymeric Hydrogels. *Small.* 2020;16(35):2002931.  
doi: 10.1002/sml.202002931
27. Xie M, Sun Y, Wang J, *et al.* Thermo-sensitive Sacrificial Microsphere-based Bioink for Centimeter-scale Tissue with Angiogenesis. *IJB.* 2022;8(4):599.  
doi: 10.18063/ijb.v8i4.599
28. Wang Y, Yue H, Liu A, *et al.* Dual crosslinkable bioink for direct and embedded 3D bioprinting at physiological temperature. *Mater Today.* 2025;85:1–16.  
doi: 10.1016/j.mattod.2025.02.005
29. Chai M, Zhong W, Yan S, *et al.* Diffusion-induced phase separation 3D printed scaffolds for dynamic tissue repair. *BMEMat.* 2024;2(3):e12108.  
doi: 10.1002/bmm2.12108
30. Wu L, Wu G, Wu D, *et al.* Stiffness-Tunable Hydrogel Microfluidic Chip Reveals the Role of Stiffness in Cholangiocarcinoma Invasion and Pre-Metastatic Niche Formation. *Adv Healthcare Mater.* 2025:e03515.  
doi: 10.1002/adhm.202503515
31. Nerger BA, Sinha S, Lee NN, *et al.* 3D Hydrogel Encapsulation Regulates Nephrogenesis in Kidney Organoids. *Adv Mater.* 2024;36(14):2308325.  
doi: 10.1002/adma.202308325
32. Yang H, Zhang J, Li Y, *et al.* Multiscale Organization of Neural Networks in a 3D Bioprinted Matrix. *Adv Sci.* 2025;12(30):e04455.  
doi: 10.1002/advs.202504455

33. Shin J, Tabatabaei Rezaei N, Choi S, Li Z, Kim D-H, Kim K. Photocrosslinkable Kidney Decellularized Extracellular Matrix-Based Bioink for 3D Bioprinting. *Adv Healthcare Mater.* 2025;14(24):2501616.  
doi: 10.1002/adhm.202501616
34. Wang C, Wang Z, Lin Y, Ouyang L. Off-the-Shelf Granular Microtissue Bioinks: Long-Term Preserved Cellularized Porous Microgels with Enhanced Cell Activity for Shelf-Ready Biofabrication. *Adv Mater.* 2025;37(44):e06616.  
doi: 10.1002/adma.202506616
35. Liu M, Jiang S, Witman N, *et al.* Intrinsically cryopreservable, bacteriostatic, durable glycerohydrogel inks for 3D bioprinting. *Matter.* 2023;6(3):983–999.  
doi: 10.1016/j.matt.2022.12.013
36. Brown NC, Ames DC, Mueller J. Multimaterial extrusion 3D printing printheads. *Nat Rev Mater.* 2025;10(11):807–825.  
doi: 10.1038/s41578-025-00809-y
37. Tarassoli SP, Jessop ZM, Jovic T, Hawkins K, Whitaker IS. Candidate Bioinks for Extrusion 3D Bioprinting—A Systematic Review of the Literature. *Front Bioeng Biotechnol.* 2021;9:616753.  
doi: 10.3389/fbioe.2021.616753
38. Miller JS, Stevens KR, Yang MT, *et al.* Rapid casting of patterned vascular networks for perfusable engineered three-dimensional tissues. *Nat Mater.* 2012;11(9):768–774.  
doi: 10.1038/nmat3357
39. Hu Y, Zhu T, Cui H, Cui H. Integrating 3D Bioprinting and Organoids to Better Recapitulate the Complexity of Cellular Microenvironments for Tissue Engineering. *Adv Healthcare Mater.* 2025;14(3):2403762.  
doi: 10.1002/adhm.202403762
40. Flégeau K, Puiggali-Jou A, Zenobi-Wong M. Cartilage tissue engineering by extrusion bioprinting utilizing porous hyaluronic acid microgel bioinks. *Biofabrication.* 2022;14(3):034105.  
doi: 10.1088/1758-5090/ac6b58
41. Lawlor KT, Vanslambrouck JM, Higgins JW, *et al.* Cellular extrusion bioprinting improves kidney organoid reproducibility and conformation. *Nat Mater.* 2021;20(2):260–271.  
doi: 10.1038/s41563-020-00853-9
42. Wu H, Xu F, Jin H, *et al.* 3D Nanofiber-Assisted Embedded Extrusion Bioprinting for Oriented Cardiac Tissue Fabrication. *ACS Biomater Sci Eng.* 2024;10(11):7256–7265.  
doi: 10.1021/acsbomaterials.4c01611
43. Bera AK, Rizvi MS, Kn V, Pati F. Engineering anisotropic tissue analogues: harnessing synergistic potential of extrusion-based bioprinting and extracellular matrix-based bioink. *Biofabrication.* 2025;17(1):015003.  
doi: 10.1088/1758-5090/ad86ec
44. Han J, Jeong H-J, Choi J, *et al.* Bioprinted Patient-Derived Organoid Arrays Capture Intrinsic and Extrinsic Tumor Features for Advanced Personalized Medicine. *Adv Sci.* 2025;12(20):2407871.  
doi: 10.1002/advs.202407871
45. Yogeshwaran S, Goodarzi Hosseinabadi H, Gendy DE, Miri AK. Design considerations and biomaterials selection in embedded extrusion 3D bioprinting. *Biomater Sci.* 2024;12(18):4506–4518.  
doi: 10.1039/D4BM00550C
46. Gupta D, Derman ID, Xu C, Huang Y, Ozbolat IT. Droplet-based bioprinting. *Nat Rev Methods Primers.* 2025;5(1):25.  
doi: 10.1038/s43586-025-00394-y
47. Hwang S, Yang K, Yoon HS, Roh YH. 3D printed pectin–chitosan polyelectrolyte hydrogels for controlled gastrointestinal release and colon-targeted delivery. *Carbohydr Polym.* 2025;376:124802.  
doi: 10.1016/j.carbpol.2025.124802
48. Yoon WH, Lee H-R, Kim S, *et al.* Use of inkjet-printed single cells to quantify intratumoral heterogeneity. *Biofabrication.* 2020;12(3):035030.  
doi: 10.1088/1758-5090/ab9491
49. Liu H, Tao T, Gan Z, *et al.* Organoid in droplet: Production of uniform pancreatic cancer organoids from single cells. *Mater Today Bio.* 2025;32:101765.  
doi: 10.1016/j.mtbio.2025.101765
50. Zhao Y, Paul R, Li Q, *et al.* DOSS: Microfluidic engineered system enables automated intelligent sorting and chemoevaluation of droplet-based colorectal adenocarcinoma organoids. *Chem Eng J.* 2025;522:166597.  
doi: 10.1016/j.cej.2025.166597
51. Yang H, Li J, Zheng Y, *et al.* Ultra-small tissue-compatible organoid printer for rapid and controllable modeling of respiratory organoids. *Device.* 2024;2(8):100420.  
doi: 10.1016/j.device.2024.100420
52. Gu Z, Fu J, Lin H, He Y. Development of 3D bioprinting: From printing methods to biomedical applications. *Asian J Pharm Sci.* 2020;15(5):529–557.  
doi: 10.1016/j.ajps.2019.11.003
53. Singh YP, Moses JC, Kim MH, *et al.* Three-tier framework for high-throughput biofabrication: Integrating 3D bioprinting, assistive platforms, and translational opportunities. *Bioact Mater.* 2026;57:726–753.  
doi: 10.1016/j.bioactmat.2025.11.024



54. Li Z, Chen L, Wu J, *et al.* A review of 3D bioprinting for organoids. *Med Rev.* 2025;5(4):318–338.  
doi: 10.1515/mr-2024-0089
55. Gehlen J, Qiu W, Schädli GN, Müller R, Qin X-H. Tomographic volumetric bioprinting of heterocellular bone-like tissues in seconds. *Acta Biomater.* 2023;156:49–60.  
doi: 10.1016/j.actbio.2022.06.020
56. Wang J, Wu Y, Li G, *et al.* Engineering Large-Scale Self-Mineralizing Bone Organoids with Bone Matrix-Inspired Hydroxyapatite Hybrid Bioinks. *Adv Mater.* 2024;36(30):2309875.  
doi: 10.1002/adma.202309875
57. Bernal PN, Bouwmeester M, Madrid-Wolff J, *et al.* Volumetric Bioprinting of Organoids and Optically Tuned Hydrogels to Build Liver-Like Metabolic Biofactories. *Adv Mater.* 2022;34(15):2110054.  
doi: 10.1002/adma.202110054
58. Wang M, Li W, Hao J, *et al.* Biomaterial-minimalistic photoactivated bioprinting of cell-dense tissues. *Cell.* 2025;189:1–17.  
doi: 10.1016/j.cell.2025.11.012
59. Wang D, Guo Y, Zhu J, *et al.* Hyaluronic acid methacrylate/pancreatic extracellular matrix as a potential 3D printing bioink for constructing islet organoids. *Acta Biomater.* 2023;165:86–101.  
doi: 10.1016/j.actbio.2022.06.036
60. Hasenauer A, Bevc K, McCabe MC, *et al.* Volumetric printed biomimetic scaffolds support in vitro lactation of human milk-derived mammary epithelial cells. *Sci Adv.* 2025;11(23):eadu5793.  
doi: 10.1126/sciadv.adu5793
61. Jain P, Kathuria H, Dubey N. Advances in 3D bioprinting of tissues/organs for regenerative medicine and in-vitro models. *Biomaterials.* 2022;287:121639.  
doi: 10.1016/j.biomaterials.2022.121639
62. Cidonio G, Glinka M, Dawson JI, Oreffo ROC. The cell in the ink: Improving biofabrication by printing stem cells for skeletal regenerative medicine. *Biomaterials.* 2019;209:10–24.  
doi: 10.1016/j.biomaterials.2019.04.009
63. Zhou X, Yu X, You T, *et al.* 3D Printing-Based Hydrogel Dressings for Wound Healing. *Adv Sci.* 2024;11(47):2404580.  
doi: 10.1002/advs.202404580
64. Shapira A, Dvir T. 3D Tissue and Organ Printing—Hope and Reality. *Adv Sci.* 2021;8(10):2003751.  
doi: 10.1002/advs.202003751
65. Yan J, Li Z, Guo J, Liu S, Guo J. Organ-on-a-chip: A new tool for in vitro research. *Biosens Bioelectron.* 2022;216:114626.  
doi: 10.1016/j.bios.2022.114626
66. Zhao D, Xu H, Ye Z, *et al.* Sequential-crosslinking facilitated droplet-droplet collision inkjet 3D printing of soft biomaterials. *Addit Manuf.* 2025;106:104809.  
doi: 10.1016/j.addma.2025.104809
67. Zhang P, Teng Z, Zhou M, *et al.* Upconversion 3D Bioprinting for Noninvasive In Vivo Molding. *Adv Mater.* 2024;36(14):2310617.  
doi: 10.1002/adma.202310617
68. Brassard JA, Nikolaev M, Hübscher T, Hofer M, Lutolf MP. Recapitulating macro-scale tissue self-organization through organoid bioprinting. *Nat Mater.* 2021;20(1):22–29.  
doi: 10.1038/s41563-020-00803-5
69. Xie D, Chen B, Xue Y, *et al.* Printable and biocompatible hydrogels for residual-free and high-throughput printing patient-derived organoid biochips. *Sci China Mater.* 2024;67(8):2505–2514.  
doi: 10.1007/s40843-024-2933-8
70. Corzo IJM, Fonseca JHLD, Ferman V. Optimizing biomaterial inks: A study on the printability of Carboxymethyl cellulose-Laponite nanocomposite hydrogels and dental pulp stem cells bioprinting. *Bioprinting.* 2024;43:e00358.  
doi: 10.1016/j.bprint.2024.e00358
71. Gan Z, Qin X, Liu H, Liu J, Qin J. Recent advances in defined hydrogels in organoid research. *Bioact Mater.* 2023;28:386–401.  
doi: 10.1016/j.bioactmat.2023.06.004
72. Cho Y, You J, Lee JH. Natural Polymer-Based Hydrogel Platforms for Organoid and Microphysiological Systems: Mechanistic Insights and Translational Perspectives. *Polymers.* 2025;17(15):2109.  
doi: 10.3390/polym17152109
73. Zhang Z, Zhu M, Luo H, Zeng F, Qi Z. Organoid scaffold materials: research and application. *Front Bioeng Biotechnol.* 2025;13:1637456.  
doi: 10.3389/fbioe.2025.1637456
74. Li Y, Saiding Q, Wang Z, Cui W. Engineered biomimetic hydrogels for organoids. *Prog Mater Sci.* 2024;141:101216.  
doi: 10.1016/j.pmatsci.2023.101216
75. Zhang C, Shen Y, Huang M, *et al.* Dynamic hydrogel mechanics in organoid engineering: From matrix design to translational paradigms. *Bioact Mater.* 2026;55:144–170.  
doi: 10.1016/j.bioactmat.2025.09.021
76. Luo L, Liu L, Ding Y, Dong Y, Ma M. Advances in biomimetic hydrogels for organoid culture. *Chem Commun.* 2023;59(64):9675–9686.

- doi: 10.1039/d3cc01274c
77. Hosseinzadeh B, Ahmadi M. Degradable Hydrogels: Design Mechanisms and Versatile Applications. *Mater Today Sustain.* 2023;23:100468.  
doi: 10.1016/j.mtsust.2023.100468
78. Santhamoorthy M, Kim SC. A Review of the Development of Biopolymer Hydrogel-Based Scaffold Materials for Drug Delivery and Tissue Engineering Applications. *Gels.* 2025;11(3):178.  
doi: 10.3390/gels11030178
79. Zhao G, Ge Y, Jin Y, *et al.* Research progress and potential of organoids based on biomimetic hydrogel materials. *Colloids Surf B Biointerfaces.* 2026;257:115168.  
doi: 10.1016/j.colsurfb.2025.115168
80. Jergitsch M, Sojunov R, Selinger F, *et al.* Fabrication and validation of an affordable DIY coaxial 3D extrusion bioprinter. *Sci Rep.* 2025;15(1):22978.  
doi: 10.1038/s41598-025-06478-9
81. Yang L, Shang J, Sun S, *et al.* Hierarchical Hydrogen Bond-Metal Coordination for High-Strength, High-Dissipation Elastomers over a Broad Temperature Range. *Small.* 2025;21(39):e06269.  
doi: 10.1002/sml.202506269
82. Rajabi M, McConnell M, Cabral J, Ali MA. Chitosan hydrogels in 3D printing for biomedical applications. *Carbohydr Polym.* 2021;260:117768.  
doi: 10.1016/j.carbpol.2021.117768
83. Szekalska M, Puciłowska A, Szymańska E, Ciosek P, Winnicka K. Alginate: Current Use and Future Perspectives in Pharmaceutical and Biomedical Applications. *Int J Polym Sci.* 2016;2016(1):7697031.  
doi: 10.1155/2016/7697031
84. Gao Q, Kim B-S, Gao G. Advanced Strategies for 3D Bioprinting of Tissue and Organ Analogs Using Alginate Hydrogel Bioinks. *Mar Drugs.* 2021;19(12):708.  
doi: 10.3390/md19120708
85. Levato R, Jungst T, Scheuring RG, Blunk T, Groll J, Malda J. From Shape to Function: The Next Step in Bioprinting. *Adv Mater.* 2020;32(12):1906423.  
doi: 10.1002/adma.201906423
86. Daly AC, Cuniffe GM, Sathy BN, Jeon O, Alsberg E, Kelly DJ. 3D Bioprinting of Developmentally Inspired Templates for Whole Bone Organ Engineering. *Adv Healthcare Mater.* 2016;5(18):2353–2362.  
doi: 10.1002/adhm.201600182
87. Wang S, Bai L, Hu X, *et al.* 3D bioprinting of neurovascular tissue modeling with collagen-based low-viscosity composites. *Adv Healthcare Mater.* 2023;12(25):2300004.  
doi: 10.1002/adhm.202300004
88. Kang S-M, Lee J-H, Huh YS, Takayama S. Alginate microencapsulation for three-dimensional in vitro cell culture. *ACS Biomater Sci Eng.* 2020;7(7):2864–2879.  
doi: 10.1021/acsbiomaterials.0c00457
89. Zhou Y, Gao X, Zhao M, Li L, Liu M. Three-dimensional printed sodium alginate clay nanotube composite scaffold for bone regeneration. *Compos Sci Technol.* 2024;250:110537.  
doi: 10.1016/j.compscitech.2024.110537
90. Fu Z, Ouyang L, Xu R, Yang Y, Sun W. Responsive biomaterials for 3D bioprinting: A review. *Mater Today.* 2022;52:112–132.  
doi: 10.1016/j.mattod.2022.01.001
91. Xu X, Lyu Y, Liu D, *et al.* Skin-Mountable Thermo-responsive Structured Hydrogel for Optical and Adhesion Coupled Functional Sensing. *Small.* 2025;21(7):2411808.  
doi: 10.1002/sml.202411808
92. Waidi YO, Kariim I, Datta S. Bioprinting of gelatin-based materials for orthopedic application. *Front Bioeng Biotechnol.* 2024;12:30.  
doi: 10.3389/fbioe.2024.1357460
93. Bociaga D, Bartniak M, Grabarczyk J, Przybyszewska K. Sodium Alginate/Gelatin Hydrogels for Direct Bioprinting—The Effect of Composition Selection and Applied Solvents on the Bioink Properties. *Materials.* 2019;12(17):254–271.  
doi: 10.3390/ma12172669
94. Gao T, Gillispie GJ, Copus JS, *et al.* Optimization of gelatin–alginate composite bioink printability using rheological parameters: A systematic approach. *Biofabrication.* 2018;10(3):034106.  
doi: 10.1088/1758-5090/aacdc7
95. Yue K, Santiago TD, Alvarez MM, Tamayol A, Annabi N, Khademhosseini A. Synthesis, properties, and biomedical applications of gelatin methacryloyl (GelMA) hydrogels. *Biomaterials.* 2015;73:254–271.  
doi: 10.1016/j.biomaterials.2015.08.045
96. Hull SM, Brunel LG, Heilshorn SC. 3D bioprinting of cell-laden hydrogels for improved biological functionality. *Adv Mater.* 2022;34(2):2103691.  
doi: 10.1002/adma.202103691
97. Kim SA, Lee Y, Park K, *et al.* 3D printing of mechanically tough and self-healing hydrogels with carbon nanotube fillers. *Int J Bioprint.* 2023;9(5):765.  
doi: 10.18063/ijb.765
98. Karvinen J, Kellomäki M. 3D-bioprinting of self-healing

- hydrogels. *Eur Polym J*. 2024;209:112864.  
doi: 10.1016/j.eurpolymj.2024.112864
99. Majstorović N, Zahedtalaban M, Agarwal S. Printable Poly (N-acryloyl glycinamide) Nanocomposite Hydrogel Formulations. *Polym J*. 2023;55(10):1085–1095.  
doi: 10.1038/s41428-023-00798-1
100. Wang H, Zhu H, Fu W, *et al*. A high strength self-healable antibacterial and anti-inflammatory supramolecular polymer hydrogel. *Macromol Rapid Commun*. 2017;38(9):1600695.  
doi: 10.1002/marc.201600695
101. Yang M, Chu L, Zhuang Y, *et al*. Multi-Material Digital Light Processing (DLP) Bioprinting of Heterogeneous Hydrogel Constructs with Perfusable Networks. *Adv Funct Mater*. 2024;34(32):2316456.  
doi: 10.1002/adfm.202316456
102. Ma W, Lu H, Xiao Y, Wu C. Advancing organoid development with 3D bioprinting. *Organoid Res*. 2025;1(1):025040004.  
doi: 10.36922/OR025040004
103. Zhang D, Huerta-López C, Heilshorn SC. Organoid bioprinting to pattern the matrix microenvironment. *Curr Opin Biomed Eng*. 2025;35:100607.  
doi: 10.1016/j.cobme.2025.100607
104. Huang L, Guo Z, Yang X, *et al*. Advancements in GelMA bioactive hydrogels: Strategies for infection control and bone tissue regeneration. *Theranostics*. 2025;15(2):460.  
doi: 10.7150/thno.103725
105. Ghosh RN, Thomas J, Janardanan A, Namboothiri PK, Peter M. An insight into synthesis, properties and applications of gelatin methacryloyl hydrogel for 3D bioprinting. *Mater Adv*. 2023;4(22):5496–5529.  
doi: 10.1039/D3MA00715D
106. Chalard AE, Dixon AW, Taberner AJ, Malmström J. Visible-light stiffness patterning of GelMA hydrogels towards in vitro scar tissue models. *Front Cell Dev Biol*. 2022;10:946754.  
doi: 10.3389/fcell.2022.946754
107. Loukelis K, Koutsomarkos N, Mikos AG, Chatzinikolaidou M. Advances in 3D bioprinting for regenerative medicine applications. *Regener Biomater*. 2024;11:rbae033.  
doi: 10.1093/rb/rbae033
108. Mierke CT. Bioprinting of cells, organoids and organs-on-a-chip together with hydrogels improves structural and mechanical cues. *Cells*. 2024;13(19):1638.  
doi: 10.3390/cells13191638
109. Zhou F, Hong Y, Liang R, *et al*. Rapid printing of bio-inspired 3D tissue constructs for skin regeneration. *Biomaterials*. 2020;258:120287.  
doi: 10.1016/j.biomaterials.2020.120287
110. Ma C, Hua B, Wang H, Ma T, Lv Q, Yan Z. Functionalized hydrogels of CeO<sub>2</sub> and Urolithin A synergistically scavenge ROS and activate mitophagy for cartilage repair. *Mater Today Bio*. 2026;37:102785.  
doi: 10.1016/j.mtbio.2026.102785
111. Gungor-Ozkerim PS, Inci I, Zhang YS, Khademhosseini A, Dokmeci MR. Bioinks for 3D bioprinting: an overview. *Biomater Sci*. 2018;6(5):915–946.  
doi: 10.1039/C7BM00765E
112. Cruz-Acuña R, Quirós M, Huang S, *et al*. PEG-4MAL hydrogels for human organoid generation, culture, and in vivo delivery. *Nat Protoc*. 2018;13(9):2102–2119.  
doi: 10.1038/s41596-018-0079-5
113. Lai W, Geliang H, Bin X, Wang W. Effects of hydrogel stiffness and viscoelasticity on organoid culture: a comprehensive review. *Mol Med*. 2025;31(1):83.  
doi: 10.1186/s10020-025-01131-7
114. Huang B, Kim M, Zhang P, Oduro E, Rau DA, Cai LH. Additive Manufacturing of Molecular Architecture Encoded Stretchable Polyethylene Glycol Hydrogels and Elastomers. *Adv Mater*. 2025;38:e12806.  
doi: 10.1002/adma.202512806
115. Mao L, Xarpidin B, Shi R, *et al*. Natural Enzyme-Loaded Polymeric Stealth Coating-Armed Engineered Probiotics by Disrupting Tumor Lactate Homeostasis to Synergistic Metabolism-Immuno-Enzyme Dynamic Therapy. *Adv Sci*. 2025;12(16):2417172.  
doi: 10.1002/advs.202417172
116. Luo Z, Jiang S, Wu YL, Li Z. Nanozyme-based therapeutic systems for diabetic wound treatment. *Ther Deliv*. 2023;14(3):179–182.  
doi: 10.4155/tde-2023-0008
117. Luo Z, Fan X, Chen Y, *et al*. Mitochondria targeted composite enzyme nanogels for synergistic starvation and photodynamic therapy. *Nanoscale*. 2021;13(42):17737–17745.  
doi: 10.1039/d1nr06214j
118. Luo Z, Cao Y, Liao Z, *et al*. Mitochondria-Targeted Gold Biometallization for Photoacoustically Visualized Photothermal Cancer Therapy. *ACS Nano*. 2024;18(43):29667–29677.  
doi: 10.1021/acsnano.4c08567
119. Li Z, Fan X, Luo Z, *et al*. Nanoenzyme-chitosan hydrogel complex with cascade catalytic and self-reinforced antibacterial performance for accelerated healing of diabetic wounds. *Nanoscale*. 2022;14(40):14970–14983.  
doi: 10.1039/d2nr04171e
120. Hu H, Lin Y, Yang B, *et al*. Biomimetic mineralization-inspired

- functional biomaterials: From principles to practice. *Chem Eng J*. 2025;504:158624.  
doi: 10.1016/j.cej.2024.158624
121. Fan X, Luo Z, Chen Y, *et al*. Oxygen self-supplied enzyme nanogels for tumor targeting with amplified synergistic starvation and photodynamic therapy. *Acta Biomater*. 2022;142:274–283.  
doi: 10.1016/j.actbio.2022.01.056
122. Wang Q, Luo Z, Li Z, *et al*. In-situ oxygen-supplying ROS nanopurifier for enhanced healing of MRSA-infected diabetic wounds via microenvironment modulation. *Acta Biomater*. 2025;193:334–347.  
doi: 10.1016/j.actbio.2024.12.044
123. Palani N, Mendonce KC, Syed Altaf RR, *et al*. Next-generation smart wound dressings: AI integration, biosensors, and electrospun nanofibers for chronic wound therapy. *J Biomater Sci Polym Ed*. 2025;1–51.  
doi: 10.1080/09205063.2025.2540362
124. Zheng Y, Mao L, Wang Q, *et al*. Mitochondria-Targeted ROS Scavenging Natural Enzyme Cascade Nanogels for Periodontitis Treatment via Hypoxia Alleviation and Immunomodulation. *Adv Sci*. 2025;12(29):e07481.  
doi: 10.1002/advs.202507481
125. Stepanovska J, Supova M, Hanzalek K, Broz A, Matejka R. Collagen bioinks for bioprinting: a systematic review of hydrogel properties, bioprinting parameters, protocols, and bioprinted structure characteristics. *Biomedicines*. 2021;9(9):1137.  
doi: 10.3390/biomedicines9091137
126. Shpichka A, Osipova D, Efremov Y, *et al*. Fibrin-based Bioinks: New Tricks from an Old Dog. *Int J Bioprint*. 2024;6(3):269.  
doi: 10.18063/ijb.v6i3.269
127. Li T, Ma Z, Zhang Y, *et al*. Regeneration of Humeral Head Using a 3D Bioprinted Anisotropic Scaffold with Dual Modulation of Endochondral Ossification. *Adv Sci*. 2023;10(12):2205059.  
doi: 10.1002/advs.202205059
128. Fisch P, Broguiere N, Finkielstein S, Linder T, Zenobi-Wong M. Bioprinting of Cartilaginous Auricular Constructs Utilizing an Enzymatically Crosslinkable Bioink. *Adv Funct Mater*. 2021;31(16):2008261.  
doi: 10.1002/adfm.202008261
129. Porcionatto MA. Strategies to use Fibrinogen as Bioink for 3D Bioprinting Fibrin-Based Soft and Hard Tissues. *Acta Biomater*. 2020;117:60–76.  
doi: 10.1016/j.actbio.2020.09.024
130. Yan Y, Li X, Gao Y, *et al*. 3D bioprinting of human neural tissues with functional connectivity. *Network Daily News*. 2024;31(2):260–274.e267.  
doi: 10.1016/j.stem.2023.12.009
131. Bhat SM, Badiger VA, Vasishta S, *et al*. 3D tumor angiogenesis models: recent advances and challenges. *J Cancer Res Clin Oncol*. 2021;147(12):3477–3494.  
doi: 10.1007/s00432-021-03814-0
132. Xianyu B, Xu H. Dynamic covalent bond-based materials: From construction to biomedical applications. *Supramol Mater*. 2024;3:100070.  
doi: 10.1016/j.supmat.2024.100070
133. Du W, Li H, Luo J, *et al*. Dynamic Schiff base linkage-based double-network hydrogels with injectable, self-healing, and pH-responsive properties for bacteria-infected wound healing. *Cellulose*. 2024;31(10):6373–6385.  
doi: 10.1007/s10570-024-05972-z
134. Hidaka M, Sakai S. Photo-and Schiff Base-Crosslinkable Chitosan/Oxidized Glucomannan Composite Hydrogel for 3D Bioprinting. *Polysaccharides*. 2025;6(1):19.  
doi: 10.3390/polysaccharides6010019
135. Willems C, Qi F, Trutschel M-L, Groth T. Functionalized gelatin/polysaccharide hydrogels for encapsulation of hepatocytes. *Gels*. 2024;10(4):231.  
doi: 10.3390/gels10040231
136. Zhang C, Fu Z, Liu Q, *et al*. Bioprinted M2 macrophage-derived extracellular vesicle mimics attenuate foreign body reaction and enhance vascularized tissue regeneration. *Biofabrication*. 2025;17(3):035007.  
doi: 10.1088/1758-5090/add49f
137. Wang H, Zhang J, Bai H, *et al*. 3D printed cell-free bilayer porous scaffold based on alginate with biomimetic microenvironment for osteochondral defect repair. *Biomater Adv*. 2025;167:214092.  
doi: 10.1016/j.bioadv.2024.214092
138. Maia FR, Oliveira JM, Reis RL. *Handbook of the Extracellular Matrix: Biologically-Derived Materials*. Springer; 2024.  
doi: 10.1007/978-3-031-56363-8
139. Mazzoldi EL, Gaudenzi G, Ginestra PS, Ceretti E, Giliani SC. Evaluating cells metabolic activity of bioinks for bioprinting: the role of cell-laden hydrogels and 3D printing on cell survival. *Front Bioeng Biotechnol*. 2024;12:1450838.  
doi: 10.3389/fbioe.2024.1450838
140. Cavallo A, Al Kayal T, Mero A, *et al*. Fibrinogen-based bioink for application in skin equivalent 3D bioprinting. *J Funct Biomater*. 2023;14(9):459.  
doi: 10.3390/jfb14090459
141. Guo K, van den Beucken T. Advances in drug-induced liver



- injury research: in vitro models, mechanisms, omics and gene modulation techniques. *Cell Biosci.* 2024;14(1):134.  
doi: 10.1186/s13578-024-01317-2
142. Jiao W, Shan J, Gong X, *et al.* GelMA hydrogel: A game-changer in 3D tumor modeling. *Mater Today Chem.* 2024;38:102111.  
doi: 10.1016/j.mtchem.2024.102111
143. Maisumu G, Willerth S, Nestor MW, *et al.* Brain organoids: Building higher-order complexity and neural circuitry models. *Trends Biotechnol.* 2025;43(7):1583–1598.  
doi: 10.1016/j.tibtech.2025.02.009
144. de Paula AGP, de Lima JD, Bastos TSB, *et al.* Decellularized extracellular matrix: the role of this complex biomaterial in regeneration. *ACS Omega.* 2023;8(25):22256–22267.  
doi: 10.1021/acsomega.2c06216
145. Walejewska E, Melchels FP, Paradiso A, *et al.* Tuning physical properties of GelMA hydrogels through microarchitecture for engineering osteoid tissue. *Biomacromolecules.* 2023;25(1):188–199.  
doi: 10.1021/acs.biomac.3c00909
146. Roth JG, Brunel LG, Huang MS, *et al.* Spatially controlled construction of assembloids using bioprinting. *Nat Commun.* 2023;14(1):4346.  
doi: 10.1038/s41467-023-40006-5
147. Wu M, Liu H, Zhu Y, *et al.* Bioinspired soft-hard combined system with mild photothermal therapeutic activity promotes diabetic bone defect healing via synergetic effects of immune activation and angiogenesis. *Theranostics.* 2024;14(10):4014.  
doi: 10.7150/thno.97335
148. Torras N, Zabalo J, Abril E, Carré A, García-Díaz M, Martínez E. A bioprinted 3D gut model with crypt-villus structures to mimic the intestinal epithelial-stromal microenvironment. *Biomater Adv.* 2023;153:213534.  
doi: 10.1016/j.bioadv.2023.213534
149. Xiao H, Liang Z, Gong X, *et al.* Application of instant assembly of collagen to bioprint cardiac tissues. *APL Bioeng.* 2025;9(2):026124.  
doi: 10.1063/5.0252746
150. Zhe M, Wu X, Yu P, *et al.* Recent advances in decellularized extracellular matrix-based bioinks for 3D bioprinting in tissue engineering. *Materials.* 2023;16(8):3197.  
doi: 10.3390/ma16083197
151. Hwang DG, Choi Y-m, Jang J. 3D bioprinting-based vascularized tissue models mimicking tissue-specific architecture and pathophysiology for in vitro studies. *Front Bioeng Biotechnol.* 2021;9:685507.  
doi: 10.3389/fbioe.2021.685507
152. Shin J, Tabatabaei Rezaei N, Choi S, Li Z, Kim DH, Kim K. Photocrosslinkable Kidney Decellularized Extracellular Matrix-Based Bioink for 3D Bioprinting. *Adv Healthcare Mater.* 2025;14(24):2501616.  
doi: 10.1002/adhm.202501616
153. Kim JJ, Cho D-W. Advanced strategies in 3D bioprinting for vascular tissue engineering and disease modelling using smart bioinks. *Virtual Phys Prototyp.* 2024;19(1):e2395470.  
doi: 10.1080/17452759.2024.2395470
154. Bansal AM, Horowitz LF, Yeung M, Gujral TS, Folch A. Bioprinting of microdissected tumor “cuboids” in hydrogels. *bioRxiv Preprint* posted online 2025;671932.  
doi: 10.1101/2025.09.05.671932
155. Leonardo M, Prajatelista E, Judawisastira H. Alginate-based bioink for organoid 3D bioprinting: A review. *Bioprinting.* 2022;28:e00246.  
doi: 10.1016/j.bprint.2022.E00246
156. He C, Yan J, Fu Y, Guo J, Shi Y, Guo J. Organoid bioprinting strategy and application in biomedicine: A review. *Int J Bioprint.* 2023;9(6):0112.  
doi: 10.36922/ijb.0112
157. Ren Y, Yuan C, Liang Q, *et al.* 3D Bioprinting for Engineering Organoids and Organ-on-a-Chip: Developments and Applications. *Med Res Rev.* 2025;45:1630–1650.  
doi: 10.1002/med.22121
158. Jones CFE, Di Cio S, Connelly JT, Gautrot JE. Design of an Integrated Microvascularized Human Skin-on-a-Chip Tissue Equivalent Model. *Front Bioeng Biotechnol.* 2022;10:915702.  
doi: 10.3389/fbioe.2022.915702
159. Oftadeh R, Azadi M, Donovan M, *et al.* Poroelastic behavior and water permeability of human skin at the nanoscale. *PNAS Nexus.* 2023;2(8):pgad240.  
doi: 10.1093/pnasnexus/pgad240
160. Yu S-y, Wu T, Xu K-h, *et al.* 3D bioprinted biomimetic MOF-functionalized hydrogel scaffolds for bone regeneration: Synergistic osteogenesis and osteoimmunomodulation. *Mater Today Bio.* 2025;32:101740.  
doi: 10.1016/j.mtbio.2025.101740
161. Yu B, Zhou D, Wang F, Chen X, Li M, Su J. Organoids for tissue repair and regeneration. *Mater Today Bio.* 2025;33:102013.  
doi: 10.1016/j.mtbio.2025.102013
162. Zhang C-J, Jin Z-B. Turning point of organoid transplantation: first-in-human trial of iPSC-derived retinal organoid grafting in patients with retinitis pigmentosa. *Sci China Life Sci.* 2024;67(5):1082–1084.  
doi: 10.1007/s11427-023-2531-3

163. Poling HM, Sundaram N, Fisher GW, *et al.* Human pluripotent stem cell-derived organoids repair damaged bowel in vivo. *Cell Stem Cell.* 2024;31(10):1513–1523.e1517.  
doi: 10.1016/j.stem.2024.08.009
164. Jun Y, Nguyen-Ngoc K-V, Sai S, *et al.* Engineered vasculature induces functional maturation of pluripotent stem cell-derived islet organoids. *Dev Cell.* 2025;60(18):2455–2469.  
doi: 10.1016/j.devcel.2025.04.024
165. Budharaju H, Singh RK, Kim H-W. Bioprinting for drug screening: A path toward reducing animal testing or redefining preclinical research? *Bioact Mater.* 2025;51:993–1017.  
doi: 10.1016/j.bioactmat.2025.07.006
166. Ma Y, He R, Deng B, *et al.* Advanced 3D bioprinted liver models with human-induced hepatocytes for personalized toxicity screening. *J Tissue Eng.* 2025;16:1–12.  
doi: 10.1177/20417314241313341
167. Yang J, Wang L, Wu R, *et al.* 3D Bioprinting in Cancer Modeling and Biomedicine: From Print Categories to Biological Applications. *ACS Omega.* 2024;9(44):25.  
doi: 10.1021/acsomega.4c06051
168. Jung M, Poltavets V, Skhinas JN, *et al.* High-throughput 3D engineered paediatric tumour models for precision medicine. *Mol Syst Biol.* 2025;21(12):1748–1777.  
doi: 10.1038/s44320-025-00152-y
169. Li Z, Li K, Zhang C, *et al.* Bioprinted Organoids: An Innovative Engine in Biomedicine. *Adv Sci.* 2025;12(33):e07317.  
doi: 10.1002/advs.202507317
170. Chliara MA, Elezoglou S, Zergioti I. Bioprinting on Organ-on-Chip: Development and Applications. *Biosensors.* 2022;12(12):1135.  
doi: 10.3390/bios12121135
171. Mitrofanova O, Nikolaev M, Xu Q, *et al.* Bioengineered human colon organoids with in vivo-like cellular complexity and function. *Cell Stem Cell.* 2024;31(8):1175–1186.e1177.  
doi: 10.1016/j.stem.2024.05.007
172. Li G, He J, Shi J, *et al.* Bioprinting functional hepatocyte organoids derived from human chemically induced pluripotent stem cells to treat liver failure. *Gut.* 2025;74(7):1150–1164.  
doi: 10.1136/gutjnl-2024-333885
173. Son J, Li S, Jeong W. Bioprinting Vascularized Constructs for Clinical Relevance: Engineering Hydrogel Systems for Biological Maturity. *Gels.* 2025;11(8):636.  
doi: 10.3390/gels11080636